International Journal of Modern Physics E, Vol. 10, No. 6 (2001) 405–457

SELECTED TOPICS IN HIGH ENERGY SEMI-EXCLUSIVE ELECTRO-NUCLEAR REACTIONS

MISAK M. SARGSIAN

Department of Physics, Florida International University, Miami, FL 33199, USA

Received 30 October 2001

We review the present status of the theory of high energy reactions with semi-exclusive nucleon electro-production from nuclear targets. We demonstrate how the increase of transferred energies in these reactions opens a completely new window for study of the microscopic nuclear structure at small distances. The simplifications in theoretical descriptions associated with the increase in the energies are discussed. The theoretical framework for calculation of high energy nuclear reactions based on the effective Feynman diagram rules is described in detail. The result of this approach is the generalized eikonal approximation (GEA), which is reduced to the Glauber approximation when nucleon recoil is neglected. The method of GEA is demonstrated in the calculation of high energy electro-disintegration of the deuteron and $A = 3$ targets. Subsequently, we generalize the obtained formulae for $A > 3$ nuclei. The relation of GEA to the Glauber theory is analyzed. Then, based on the GEA framework we discuss some of the phenomena which can be studied in exclusive reactions: nuclear transparency and short-range correlations in nuclei. We illustrate how light-cone dynamics of high-energy scattering emerge naturally in high energy electro-nuclear reactions.

1. Introduction

Presently, our knowledge of the microscopic structure of nuclei is limited mainly to the dynamics of single-nucleon states characterized by the momenta $\leq$ 200–250 MeV/c and excitation energies significantly smaller then the nucleon mass ($\leq$ 100 MeV). The dynamics of the nuclear structure at very short distances in which nucleons may be significantly overlapped is practically unexplored. Naive estimations indicate that such configurations may provide instantaneous hadronic densities up to four times larger than average nuclear densities, comparable to those that may occur in a neutron star. However, to provide direct access to these configurations the high momentum and energy should be transfered to the nucleus to resolve the shortest possible space-time distances of the nuclear structure. Providing large values of missing momentum and energy in these processes and using higher resolving power of the high momentum and energy transfer reactions one will be able to directly probe the short-range nucleonic correlations, which are believed to be the main source of the high-momentum component of the nuclear wave functions.

The fundamental question that these studies can answer is at which time intervals and distances the quark and gluons become the relevant degrees of freedom for multinucleon configurations at small distances — short range correlations.

Electro-nuclear reactions are best suited to high momentum and energy transfer processes since the electron coupling with the virtual photon can be precisely calculated in QED. On the other hand, the well-known fact from particle physics that with increasing energies, theoretical description of photon-hadron interactions become more simple and reliable (see e.g. Refs. 1 and 2) would also be relevant for electro-nuclear reactions.

In addition to the increase in the transfered momenta and energies, the increase in the degrees of exclusiveness of electro-nuclear reactions when more products are registered in the final state of the reaction, allows us to attain a deeper understanding of the dynamics of the reaction as well as gain more information about the microscopic structure of the short-range nucleon correlations.

The combination of these two factors — *high energy and momentum transfer* and (*semi*) *exclusiveness* of the reaction — makes electro-nuclear reactions a unique laboratory for studying nuclear quantum chromodynamics. The additional boost in popularity of high-energy semi-exclusive reactions was given by the prediction of the unique phenomenon of Color Transparency (CT), in which the dominance of small sized quark-gluon degrees of freedom in high momentum transfer eN scattering is manifested by the disappearance of the absorption of the nucleon due to the propagation in the nuclear medium.

The last decade saw a tremendous growth in the numbers of proposed and performed experiments dedicated to semi-exclusive nuclear reactions with large values of momentum transfer (≥ 1 GeV/c) (see e.g. Refs. 3–13). The experimental studies of high momentum transfer semi-exclusive reactions are an important part of the scientific programs of the high energy, high intensity electron facilities at Jefferson Lab (see e.g. Ref. 14) and HERMES (see e.g. Ref. 15). Therefore, the development of an adequate theoretical framework to describe these reactions is becoming a pressing problem.

The major issue facing the theoretical description of semi-exclusive reactions is that when the final state of the reaction in addition to the scattered electron consists of at least one hadron the strong reinteraction of the produced hadrons in the nuclear environment becomes the dominant feature of these reactions.

One of the issues in describing these reinteractions is that the theoretical methods which were successful in medium-energy nuclear physics should be upgraded in order to describe hadronic reinteractions in the processes in which energies transferred to a nuclear target are large ($\gtrsim$ a few GeV).

At the energies of the produced hadronic system $E_N \leq 1$ GeV the final state interactions in semi-exclusive nuclear reactions are usually evaluated in terms of an effective potential for the interaction in the residual system — the optical model approximation (see, for example, Ref. 16). Two important features of high-energy FSI make the extension of the potential formalism to high energies problematic.

Firstly, the number of essential partial waves increases rapidly with the energy of the $N(A-1)$ system. Secondly, the NN interaction which is practically elastic for $E_N \leq 500$ MeV becomes predominantly inelastic for $E_N > 1$ GeV. Hence, the problem of scattering can hardly be treated as a many body quantum mechanical problem. Introducing in this situation a predominantly imaginary potential to account for hadron production is not a well-defined mathematical concept. So, theoretical methods successful below 1 GeV become ineffective at the transferred momenta which can be reached at Jefferson Lab[17] and HERMES.[18]

Final state reinteraction in hadron induced nuclear reactions at higher energies ($E_N > 1$ GeV) are often described within the approximation of the additivity of phases, acquired in the sequential rescatterings of high-energy projectiles off the target nucleons (Glauber model[19]). This approximation made it possible to describe the data on elastic hA scattering at hadron energies 1 GeV $< E_h <$ 10–15 GeV (cf. Refs. 20–22).

There have been many theoretical works in the last several years where the same principle of Glauber rescattering has been applied to the description of the cross-sections of $A(e,e'N)(A-1)$ reactions.[23–36] Many of these works discussed the reactions in which the cross-sections were integrated over the excitation energies of the residual nuclear system and the kinematics were restricted to small momenta of the residual system, $\mathbf{p}_{A-1} \leq p_{\mathrm{F}}$, where $p_{\mathrm{F}} \approx 250$ MeV/c is the characteristic Fermi momentum of the nuclear system.

In Refs. 37 and 38 the cross-section of $A(e,e'N)(A-1)$ reactions has been calculated for small excitation energies that are characteristic for particular shells of a target nucleus with $A \gtrsim$ 12–16.

In all these cases the Glauber approximation, which considers the nucleons in the nuclei as stationary scatterers, was a good approximation. The theoretical generalization for electro-production reactions was rather straightforward, which mainly accounted for the fact that energetic hadrons originate from the point of virtual-photon-nucleon interaction (but not from $-\infty$ as was the case in hA reactions).

However, the Glauber approximation cannot be applied to the class of eA reactions in which the main emphasis is given to the high momentum of the bound nucleon and the high excitation energies of the residual nuclei. This situation is especially important in studies of short-range nuclear properties in which large values of missing momentum and excitation energy are involved. It is also important in studies on the transparency of the nuclear medium for high momentum transfer electro-production reactions.

This review focuses on the development of the theoretical framework of calculation of the final state interactions (FSI) at high energy and momentum transfer (hard) semi-exclusive $A(e,e'N)X$, $A(e,e'NN)X$ reactions, with states X representing ground or excited states of the residual nucleus. We will concentrate on the kinematical region where the bound nucleon momenta and excitation energies in the nuclear system are large enough that short-range multinucleon correlations are

expected to be dominant in the nuclear wave function. We are particularly interested in the region of the transfered four-momenta $1 \leq Q^2 \leq 6$ GeV^2. Here the lower limit is defined from the condition that the knocked-out hadronic system is energetic enough that the high energy approaches become applicable. The upper limit is defined from the conditions that color coherence effects are small and the produced hadronic state represents the single state (e.g. nucleon) but not the superposition of different hadronic states (wave packet) (see e.g. Ref. 39). Additionally, the upper limit of Q^2 restricts the energies of rescattering nucleons, $E \leq 10$–15 GeV. The last condition makes the ratio of the inelastic diffractive cross-section to the elastic cross-section in the soft hadronic interactions a small correction. As was demonstrated by Gribov,[40] the smallness of this ratio is a necessary condition for Glauber type approximations to be a legitimate approximation. Thus, we have a unique kinematic window where the theoretical methods of high energy scattering may have a simpler realization due to the fact that mainly diagonal (elastic) terms in hh rescattering will contribute. Within this kinematic window, we will discuss the apparatus of the derivation and application of the developed generalized eikonal approximation (GEA) to the various types of semi-exclusive high energy eA reactions.

The paper is organized as follows. In Sec. 2 the general kinematic requirements are discussed. The emergence of the new type of small parameter in the problem is explained. In Sec. 3 we elaborate on the basic types of the mechanisms that contribute to the semi-exclusive electro-nuclear reactions. The high energy properties of impulse approximation in eA reactions are considered in Sec. 4. It is demonstrated that for the selected components of electromagnetic current the off-shell effects in the bound nucleon spinors do not contribute. In Sec. 5 we discuss high energy properties of exchange currents. Although it is impossible to do self-consistent quantitative calculations, it is still possible to demonstrate based on the general principles that with the increase of the transferred momenta and energy the exchange currents will be suppressed as compared to the impulse approximation. In Sec. 6 we discuss the final state interactions in semi-exclusive reactions and their important features in the high energy limit. The basic points here are the emergence of the approximate conservation law and the reduction theorem which allows us to sum potentially infinite number of rescattering diagrams into the final set of Feynman diagrams. The effective Feynman rules which allow us to calculate the high energy n-fold rescattering amplitude are defined in Sec. 7. These rules constitute the basis of GEA. In Sec. 8 we demonstrate the application of the Feynman rules to the reaction of high energy electrodisintegration of the deuteron. The GEA calculations are compared with the conventional Glauber approximation as well as with the calculation based on the intermediate energy approach. The application of the electrodisintegration reaction for the studies of color coherence phenomena in the double scattering regime is discussed as well. The analysis of high energy electrodisintegration of the $A = 3$ targets and further elaboration of the difference between GEA and conventional Glauber approximation are discussed in Sec. 9. In Sec. 10 the developed formalism is related to the studies of short-range correlations

in the nuclei. The relation of the GEA to the description of scattering amplitudes on the light cone is discussed in Sec. 11. Section 12 contains the conclusions of the review. In Appendix A we demonstrate why the closure approximation in general is applicable in the light cone but not in the nucleus rest frame at large values of missing momenta and energies. The details of the derivation of the rescattering amplitude in the $d(e,e'N)N$ reaction is given in Appendix B.

2. General Kinematic Requirements, Emergence of Small Parameters

We start by considering the general type of reactions, Fig. 1, in which high momentum $q \equiv (q_0, \mathbf{q})$ is transferred to the nucleus. The main feature of the final state in these reactions is that it contains the fast hadron that carries almost the entire momentum of the virtual photon $\mathbf{p_f} \approx \mathbf{q}$, with $|\mathbf{q}| \sim$ several GeV/c. All other hadrons (p_s) in the final state have relatively low energy ($p_s \sim$ hundreds of MeV/c).

Thus, the major kinematic requirement is

$$\begin{aligned} Q^2 = \mathbf{q^2} - q_0^2 > 1 \text{ GeV}^2\,, \qquad & \mathbf{p_f} \approx \mathbf{q}\,, \\ p_f \gg p_m, p_s \sim \text{a few hundred MeV}/c\,, \qquad & E_f \gg E_m = E_f - q_0\,, \end{aligned} \tag{1}$$

where $\mathbf{p_m} = \mathbf{p_f} - \mathbf{q}$ is the missing momentum of the reaction, $E_f = \sqrt{m^2 + p_f^2}$ and E_m characterizes the excitation of the residual nuclear system, m is the mass of the nucleon. Note that our definition of E_m differs from the often used definition of missing energy in which the kinetic energy of the center-of-mass of the $A-1$ system is subtracted. However, for our discussion this difference is not important.

Now, if one constructs the $\pm$ components of four-momenta (which correspond to the energy and longitudinal momentum of the particle in the light-cone

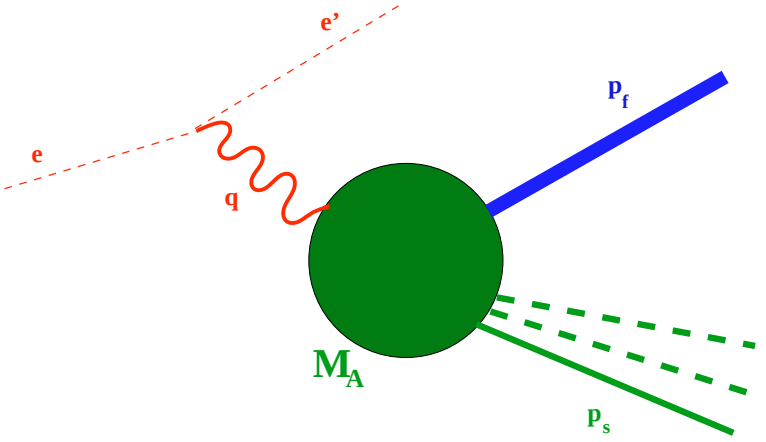

Fig. 1. General diagram.

reference frame):

$$p_\pm = p_0 \pm p_z\,, \tag{2}$$

where the z-direction is defined by the direction of virtual photon momentum $\mathbf{q}$, then one observes that the condition of Eq. (1) corresponds to the smallness of the following combinations:

$$\frac{q_-}{q_+} \approx \frac{mx}{2q} \ll 1 \quad \text{and} \quad \frac{p_{f-}}{p_{f+}} \approx \frac{m^2}{4p_f^2} \ll 1\,, \tag{3}$$

where $x = Q^2/2mq_0$. The availability of these *small parameters* is one of the important features of high energy scattering compared to low-intermediate energy reactions. We will see below how these conditions will simplify the theoretical treatment of semi-exclusive eA reactions.

Some useful rules: Throughout this review we may use dot-product rules which apply to the light-cone momentum definition of $p_\pm$. The four-momentum has two equivalent ways for the representation $p^\mu = (p_0, p_z, p_\perp) = (p_+, p_-, p_\perp)$ and the scalar product of two four-vectors is defined as

$$p_1 \cdot p_2 \equiv p_{10}p_{20} - p_{1z}p_{2z} - p_{1\perp}p_{2\perp} = \frac{1}{2}p_{1+}p_{2-} + \frac{1}{2}p_{1-}p_{2+} - p_{1\perp}p_{2\perp}\,. \tag{4}$$

3. Some Basic Features of Semi-Exclusive Electro-Nuclear Reactions

The first semi-exclusive electro-nuclear reactions, which have been studied at intermediate energies, confirmed the expectations that the complexity of hadronic systems significantly restricts the unambiguous treatment of underlying dynamics of the reaction. In general, four main processes contribute to the semi-exclusive electro-nuclear reactions (Fig. 2) in which at least one energetic nucleon is registered in the final state:

- Impulse approximation (IA) amplitude (Fig. 2(a)), in which the virtual photon knocks-out the bound nucleon, which propagates to the final state without further interactions
- Final state interaction (FSI) amplitude (Fig. 2(b)), in which the knocked-out nucleon reinteracts with the residual hadronic system
- Amplitude with meson exchange currents (MEC) (Fig. 2(c)), in which the virtual photon interacts with the exchanged (between two-nucleon system) mesons
- Isobar current contribution amplitude (IC) (Fig. 2(d)), in which the virtual photon produces Δ-isobar which reinteracts with the residual nuclear system producing the final hadronic state

The study of the small distance properties of nuclei in these reactions is related to the exploration of IA diagrams at high values of missing momenta and energy. However, in such kinematics at small Q^2 ($\ll 1$ GeV^2), in practically all cases the FSI, MEC and IC give dominant contributions.[41–43]

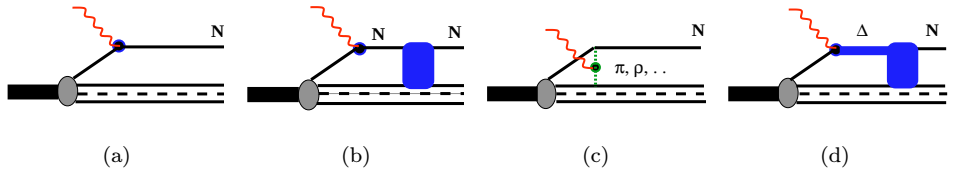

Fig. 2. (a) Impulse Approximation, (b) final state interaction, (c) meson exchange and (d) Δ-isobar contribution diagrams.

There are several reasons for the dominance of FSI, MEC and IC diagrams in the kinematics of large missing momentum p_m, missing energy E_m and low Q^2. While at large p_m and E_m the IA amplitude is defined by the nuclear wave function at short inter-nucleon distances, the FSI, MEC and IA amplitudes are defined by nuclear wave functions of average configurations.

The dominance of MEC and IC amplitudes follows also from kinematical considerations that at small Q^2 high missing momenta p_m in semi-exclusive $A(e,e'N)X$ reactions can be observed only at $x < 1$, i.e. in the kinematic region close to the pion threshold. It can be seen from Fig. 3, where we calculated the p_{mz} dependence on x for the quasi-elastic $e + d \to e' + p + n$ reaction that at $Q^2 < 1$ GeV^2 only $x < 1$ is appropriate for detection of large $p_{mz} \geq 300$ MeV/c.

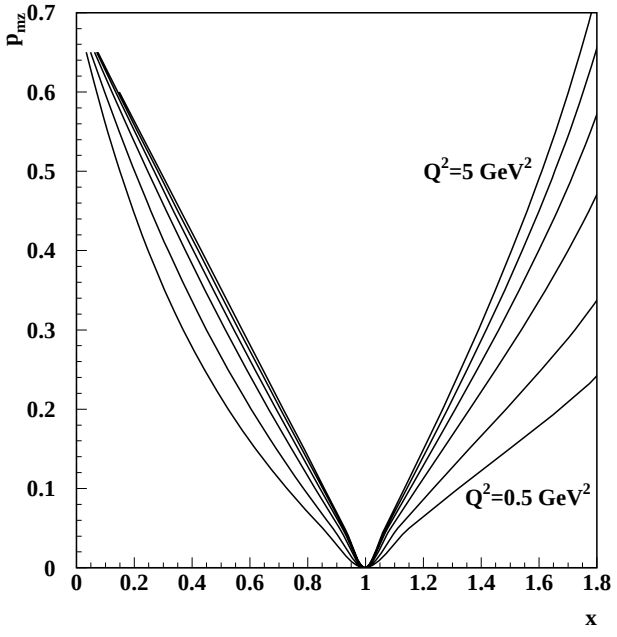

Fig. 3. The $|p_{mz}|$ as a function of x, for different values of Q^2, for the quasielastic $d(e,e'N)N$ reaction. The lines between $Q^2 = 0.5$ and $Q^2 = 5$ GeV^2 curves correspond to the values of $Q^2 = 1, 2, 3, 4$ GeV^2.

As to the final state interactions at small Q^2, they are dominated by S wave scattering and have broad angular distributions. Thus, there exists no clear criteria on how to isolate or suppress FSI with respect to PWIA.

In general terms the dominance of FSI, MEC and IA amplitudes indicates the impossibility of probing small space-time intervals in the nucleus using probes of larger size ($1/q \geq 1$ fm).

In Fig. 4 we present the typical intermediate energy measurement, which demonstrates how large MEC and IC contributions are in the cross section at large missing momenta and low Q^2. The calculations in the kinematic region of these experiments show that at large p_m MEC and IC significantly dominate the PWIA contribution.

With the increase in energies, the situation changes qualitatively. It may sound paradoxical, but at high energy transfer, when the wavelength of the probe becomes much smaller than the sizes of interacting particles, the situation becomes simpler. Using the example presented by Cheng and Wu,[2] comparison of the low energy with the high energy cases is analogous to the situation when one explores the room and

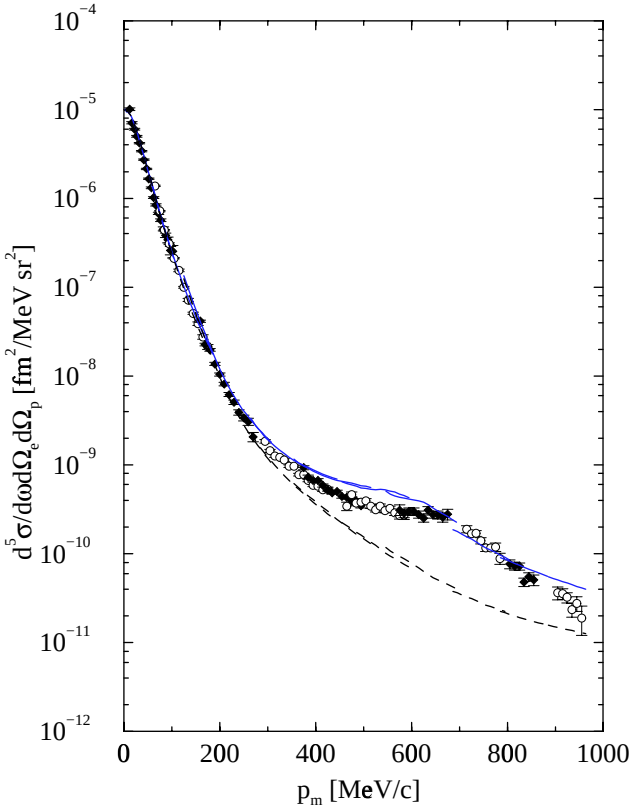

Fig. 4. The p_m dependence of the differential cross sections of $d(e,e'p)n$ reactions at $Q^2 = 0.13$–0.33 GeV^2. The data are from Ref. 42. Solid and dashed lines correspond to the calculations of Arenhövel[44] with and without MEC and IC contributions, respectively.

in one instance the shapes of the objects in the room will change with the color of the light one uses to look at the objects (long wavelength case) compared to the case when the shapes of the objects are independent of the color of the light (short wavelength case).

Mathematically, the first qualitative change we encounter with increasing energies is the availability of small parameters discussed in Sec. 2. As we will see later, the existence of these small parameters in the situation when interactions are strong plays an important role in the calculation of these reactions.

Next, we consider the basic features of all of four amplitudes in Fig. 2 at large values of Q^2. The impulse approximation, meson exchange currents and isobar contributions will be considered briefly, discussing only the qualitative features of these amplitudes at high energies. Their detailed discussion is beyond the scope of the present review. The final state interaction will be considered in detail with the derivation of effective Feynman rules of n-fold rescattering amplitude.

4. Impulse Approximation Diagrams

We start by considering the simplest case of electro-disintegration of the deuteron, Fig. 5, in which $e+d \to e'+p+n$ scattering with the recoil nucleon momenta $p_s \sim$ a few hundred MeV/c corresponds to the virtual photon interaction with the bound nucleon of Fermi momenta $-\mathbf{p_s}$. Choosing the momentum of the bound nucleon large enough that it can no longer be described as quasifree, we restrict however the upper limit of this momentum (≤ 600 MeV/c) so that the nucleonic degrees of freedom are still relevant for the bound system. Description of the electromagnetic interaction with bound (off-shell) nucleons possesses many theoretical uncertainties, related to the absence of a self-consistent theory of strong interaction that describes the binding of the nucleon. The origin of the off-shell effects in $\gamma^* N_{\rm bound}$ scattering amplitude is somewhat different for low and high energy domains. In the case of low energy transfer the nucleons represent the quasiparticles whose properties are modified due to the in-medium nuclear potential (see e.g. Ref. 45). At high Q^2 the virtual photon interacts with nucleons and the phase volume of the process is sufficiently large. As a result, the off-shell effects in the high energy limit are mostly related to the non-nucleon degrees of freedom. To demonstrate this transition, as

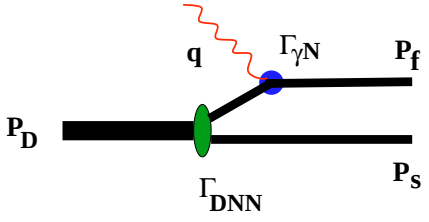

Fig. 5. Impulse approximation diagram for $e + d \to e' + p + n$ scattering.

an example we discuss the problem of off-shellness related to the description of the bound nucleon spinors.[a]

The covariant Feynman amplitude corresponding to the diagram in Fig. 5 can be written as

$$A_0^\mu = -\frac{\bar{u}(p_s)\bar{u}(p_f)\Gamma^\mu_{\gamma^* N}\cdot[\hat{p}_D - \hat{p}_s + m]\cdot\Gamma_{DNN}}{(p_D - p_s)^2 - m^2 + i\epsilon}\,. \tag{5}$$

Here, we used the notation $\hat{p} \equiv p_\mu\gamma^\mu$ and for simplicity suppressed the spin indices of the deuteron. Γ_{DNN} represents the covariant $D \to NN$ transition vertex and $\Gamma^\mu_{\gamma^* N}$ is the covariant electromagnetic vertex of the $\gamma^* N_{\rm bound} \to N$ transition. Note that both Γ_{DNN} and $\Gamma^\mu_{\gamma^* N}$ are the covariant vertices and in the time ordered expansion they contain both impulse approximation and vacuum fluctuation diagrams (e.g. Γ_{DNN} may represent $\bar{N}D \to N$ and $\Gamma^\mu_{\gamma^* N}$ may represent $\gamma^* \to \bar{N}N$). The lack of the self-consistent theory of strong interaction in the strong QCD regime does not allow us to calculate both vertices from first principles.

Furthermore, we will discuss only the "$\mu = -$" component of the electromagnetic current, highlighting its several important features in the limit of $\mathcal{O}(q_-/q_+)$. First, for the "$-$" component of the electromagnetic current, the vacuum component of the $D \to NN$ vertex is negligible. This is true if the covariant amplitude is calculated in the reference frame in which the target (deuteron) has a very large (infinite) momentum (or in the light cone reference frame) (see e.g. Ref. 47). In this reference frame, for the "$-$" component, the contribution from the amplitude of the $\gamma^* \to N\bar{N}$ transition with subsequent $\bar{N}d \to N$ interaction is strongly suppressed and only the contribution in which γ^* interacts with the bound nucleon survives. Note that this is not true for the other components of electromagnetic currents. In general, the complete description of the off-shell nucleon currents requires the negative energy state contribution with additional invariant form-factors as compared to the on-shell nucleon (see e.g. Ref. 48).

The next question is how well we can identify the $\gamma^* N_{\rm bound}$ scattering in the A_0^- amplitude of Eq. (5), with the virtual photon scattering off a free nucleon spinor. For this we observe that the propagator of bound nucleon in Eq. (5) can be written as

$$\hat{p}_D - \hat{p}_s + m = (\hat{p}_D - \hat{p}_s + m)^{\rm on} + \frac{1}{2}[(p_D - p_s)^{\rm off}_+\gamma_- - (p_D - p_s)^{\rm on}_+\gamma_-]\,, \tag{6}$$

where "on" and "off" superscripts refer to the on-shell and off-shell components of the momentum, respectively. In the derivation of Eq. (6) we added and subtracted the term $\frac{1}{2}(p_D - p_s)^{\rm on}_+\gamma_-$ to construct the completely on-shell nucleon propagator. Using now the kinematic relations

$$(p_D - p_s)^{\rm on} = \frac{m^2 + (p_D - p_s)^2_\perp}{(p_D - p_s)_-}$$

[a]Transition from the quasiparticle to nucleon picture of the eA interaction could give also a natural explanation for the recently observed disappearance of quenching at high values of Q^2.[46]

and

$$(p_D - p_s)^{\rm off} = \frac{(p_D - p_s)^2 + (p_D - p_s)_\perp^2}{(p_D - p_s)_-}\,, \tag{7}$$

which are based on the mass relation formula $p_+p_- - p_\perp^2 = p^\mu p_\mu$, and expressing the on-shell propagator through the sum of the on-shell spinors as

$$(\hat{p}_D - \hat{p}_s + m)^{\rm on} = \sum_\lambda u_\lambda(p_D - p_s)\bar{u}_\lambda(p_D - p_s)\,, \tag{8}$$

for Eq. (6) one obtains

$$\hat{p}_D - \hat{p}_s + m = \sum_\lambda u_\lambda(p_D - p_s)\bar{u}_\lambda(p_D - p_s) + \frac{(p_d - p_s)^2 - m^2}{2(p_D - p_s)_-}\gamma_-\,. \tag{9}$$

Inserting Eq. (9) into Eq. (5), for the "$-$" component of A_0^μ one obtains

$$A_0^- \equiv A_0^{{\rm on},-} + A_0^{{\rm off},-} = -\sum_\lambda \frac{\bar{u}(p_s)j^-(Q^2)\bar{u}(p_D - p_s)\Gamma_{DNN}}{(p_D - p_s)^2 - m^2 + i\epsilon} - \frac{\bar{u}(p_s)\bar{u}(p_f)\Gamma^-_{\gamma^*N}\cdot\gamma^-\Gamma_{DNN}}{2(p_D - p_s)_-}\,. \tag{10}$$

To illustrate the suppression of the contribution of off-shell effects in the spinor structure of A_0^- we shall compare $A_0^{{\rm off},-}$ with $A_0^{{\rm on},-}$. For this, we assume the following analytic form of the nucleon electromagnetic vertex:

$$\Gamma^\mu_{\gamma^*N} \sim A\cdot\gamma^\mu + B\cdot\sigma^{\mu,\nu}q^\nu\,, \tag{11}$$

where A and B are functions of scalar combinations of q^μ, p_f^μ and $(p_D - p_s)^\mu$. Using this form and the identity $\gamma_-\gamma_- = 0$ one can estimate that

$$\frac{A_0^{{\rm off},-}}{A_0^{{\rm on},-}} \approx \mathcal{O}\left(\frac{q_-}{q+}\right) \ll 1\,. \tag{12}$$

Therefore, for the "$-$" component of the IA amplitude the off-shell part in the nucleon spinors decreases with the increase of transferred energy. Notice that the "$-$"component of the current in particle physics is usually called a "good" component of the current (see e.g. Ref. 49). It can be unambiguously identified in electro-nuclear reactions (for example, in the inclusive $A(e,e')X$ reactions the structure function $W_2 \sim |A_0^-|^2$).

The conclusion of the above discussion is that in the high energy limit one can identify the "good" component of electromagnetic current which is insensitive to the off-shellness of the bound nucleon spinor. In this limit, for the IA term, one obtains

$$A_0^- \approx \psi_D(p_m)\cdot J_N^-(Q^2, p_f, p_m)\,, \tag{13}$$

where $\mathbf{p_m} = \mathbf{p_D} - \mathbf{p_s} = \mathbf{p_f} - \mathbf{q}$ and $\psi_D(p_m)$ is the wave function of the deuteron defined in the reference frame where the deuteron is fast (or in the light-cone). Thus, the price we pay for gaining the simplicity in the description of electromagnetic current is the necessity to calculate the nuclear wave functions in the light-cone reference frame (see e.g. Refs. 47).

It is worth noting that in the nuclear rest frame one can identify the $\Gamma^{\mu}_{\gamma^* N}$ vertex with nonrelativistic wave function (see e.g. Ref. 50) and electromagnetic current with the positive energy nucleon spinors (see e.g. Ref. 51) only in the limit of $\mathcal{O}(p_s^2/m^2)$. Behind this limit in the nuclear rest frame description, there is no defined strategy to discriminate between on- and off-shell contributions of electromagnetic current (for discussions see Refs. 52 and 53).

It should be emphasized that the above discussion on off-shellness is relevant only for the situations in which the nucleons are the relevant degrees of freedom. At the transferred energies when nucleon substructure plays a dominant role, a different type of off-shellness related to the medium modification of quark-gluon distributions emerges (e.g. EMC effects in deep-inelastic eA scattering).

5. Meson Exchange Currents and Isobar Contributions

Next, we consider the contributions of MEC and IC amplitudes in the high energy limit of Sec. 2 (Eq. (1)). Since both MEC and IC are two-body currents, it is sufficient to consider the deuteron target (Fig. 6) to arrive at the general conclusion.

The experimental results at low Q^2 $d(e,e'N)N$ data demonstrated that with an increase of p_m the MEC and IC contributions become dominant. However, one again expects major qualitative changes with the increase of Q^2 (≥ 1 GeV^2).

The major problem we face in the estimation of MEC at high energies is that with an increase of Q^2 the virtuality of exchanged mesons in Fig. 6(a) grows and $Q^2 \gg m^2_{\rm meson}$. (As was noted by Feynman, "*a pion far off its mass shell* may be a meaningless — or at least a highly complicated — idea".[1])

However, theoretically from very general principles, one expects that the contribution of meson exchange currents will decrease with an increase in the virtuality of the exchanged photon, $-Q^2$. Indeed it can be shown that MEC diagrams (Fig. 6(a)) have an additional $\sim 1/Q^4$ dependence as compared to the IA diagrams

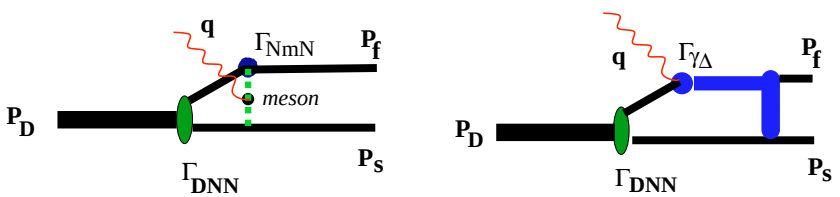

(a) (b)

Fig. 6. Meson Exchange Current and Δ-isobar contribution amplitudes for the $e + d \to N + N$ reaction.

of Fig. 5). This suppression comes from two major factors. First, since at the considered kinematics the knocked-out nucleon is fast and takes almost the entire momentum of the virtual photon q, the exchanged meson propagator is proportional to $(m^2_{\rm meson}+Q^2)^{-1}$. Secondly, an additional Q^2 dependence comes from the NN–meson form-factor $\sim (1+Q^2/\Lambda)^{-2}$. Thus, overall the Q^2 dependence of MEC amplitude can be estimated as

$$A^{\mu}_{\rm MEC} \sim \int d^3p\cdot\Psi(p)\frac{J^{\mu}_m(Q^2)}{(Q^2+m^2_{\rm meson})}\Gamma_{MNN}(Q^2)$$

$$\propto \int d^3p\cdot\Psi(p)\left(\frac{1}{(Q^2+m^2_{\rm meson})^2(1+Q^2/\Lambda^2)^2}\right), \qquad (14)$$

where $J^{\mu}_m(Q^2)$ is the meson electromagnetic current proportional to the elastic form factor of the meson $\sim \frac{1}{Q^2+m^2_{\rm meson}}$, $m_{\rm meson}\approx 0.71$ GeV and $\Lambda\sim 0.8$–1 GeV^2.[b] Comparing Eq. (14) with Eq. (13) we can estimate the overall additional Q^2 dependence as compared to IA contribution as $\sim (1+Q^2/\Lambda^2)^{-2}$, which is a rather conservative estimation (see the footnote on this page). Thus, one expects that MEC contributions will be strongly suppressed as soon as $Q^2\geq (m^2_{\rm meson},\Lambda)\sim 1$ GeV^2. The indication of such suppression is clearly seen in the SLAC experiment,[55] where the ratios of structure functions, W_1/W_2 are measured at the deuteron threshold $x\to 2$. Since in the limit of $x\to 2$ one expects the dominance of MEC[55] (meson exchanges needed to provide the bound pn final state), the Q^2 dependence of this ratio at fixed relative energy of final pn system will be very sensitive to the Q^2 dependence of MEC contributions.

As an experimental indication of MEC suppression at high Q^2 in Fig. 7 we demonstrate the Q^2 dependence of W_1/W_2 for different values of E_{pn}. Note that $E_{pn}=0$ corresponds to the deuteron threshold where MEC should be especially enhanced. The figure clearly indicates that MEC contribution decreases as Q^2 increases and additionally it indicates that starting at $E_{pn}\geq 50$ MeV, MEC contribution becomes negligible in the $Q^2\geq 1.5$ GeV^2 region.

For the case of IC contribution, similar to the consideration of MEC, we are interested mainly in the energy dependence of scattering amplitude compared to the IA amplitude, A_0. For this, it is sufficient to observe that one can estimate the scattering amplitude of Fig. 6(b) as follows:

$$A^{\mu}_{\rm IC}\sim i\int \psi_D\left(p_{mt}-k_t,p_{mz}-\frac{m^2_{\Delta}-m^2}{2q}\right)J_{\gamma^*N\Delta}(Q^2)A_{\Delta,N\to NN}(k_t)d^2k_t\,, \quad (15)$$

[b]We assume here that different meson-nucleon vertices have similar dependencies on the virtuality, assume the dipole dependence on the virtuality which corresponds to the neglecting of the size of a meson compared to the baryon size (for large Q^2 quark counting rules lead to $\Gamma_{MNN}(Q^2)\sim 1/Q^6$), and use restrictions on the Q-dependence of the πNN vertex from the measurement of the anti-quark distribution in nucleons (for a recent discussion see Ref. 54).

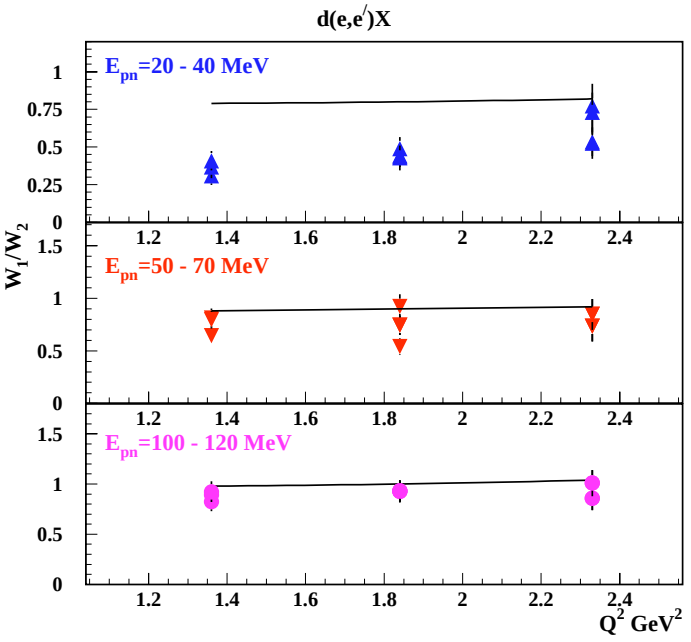

Fig. 7. The Q^2 dependence of W_1/W_2 from inclusive $d(e,e')X$ reaction. The data are from Ref. 55. E_{pn} $(= W_{pn} - m_D - \epsilon_d^{\rm bound})$, where $W_{pn}^2 = W_{\gamma^* D}^2 = (q^\mu + p_D^\mu)^2$, is the C.M. energy of the proton and neutron in the final state of the reaction. Solid lines are PWIA predictions within light-cone dynamics by a collinear approach.[56,101]

where $J_{\gamma^* N\Delta}(Q^2)$ and $A_{\Delta,N\to NN}$ are the electromagnetic $N \to \Delta$ and hadronic $N\Delta \to NN$ transition amplitudes, respectively. Comparing $A_{\rm IC}$ with A_0 of Eq. (13) one first observes that the $x < 1$ and $x > 1$ regions at the same $|p_m|$ have a different contributions from the intermediate Δ excitations. It can be seen from Eq. (15) that the amplitude of IC contribution is proportional to

$$\psi_D \left(p_{mt} - k_t, p_{mz} - \frac{m_\Delta^2 - m^2}{2q} \right) , \tag{16}$$

where p_{mt} and p_{mz} are the transverse and longitudinal components of the measured missing momentum. The Eq. (15) shows that one has more IC contribution in the $x < 1$ region than in the $x > 1$ region since in the first case $p_{mz} - [(M_\Delta^2 - M_N^2)/2q] < p_{mz}$, while for $x > 1$, $|p_{mz} - [(M_\Delta^2 - M_N^2)/2q]| > |p_{mz}|$.

Therefore, the access to the $x > 1$ region at high Q^2 (Fig. 3) allows us to separate regions where the IC contribution is suppressed kinematically as compared to the IA contribution.

Another possible suppression comes from the comparison of elastic $J^\mu_{\gamma^* N}$ and Δ transition $J_{\gamma^* N\Delta}$ currents. Such a suppression at high Q^2 is expected from perturbative QCD arguments, since Δ represents a helicity-flip transition which is suppressed in the domain of pQCD. The hypothesis of the smooth matching of nonperturbative and perturbative regimes of QCD suggests that the suppression

of helicity flip amplitudes should already be observed at relatively high $Q^2 \geq$ a few GeV^2. Indeed the experimental data on elastic and transition form factors suggest such a suppression.[57]

Finally, the additional suppression of the IC contribution comes from the energy dependence of the $A_{\Delta,N\to NN}$ amplitude. To estimate the energy dependence of this amplitude, one observes that the Feynman amplitude of the scattering process which proceeds by an exchange of particle with spin J behaves as $A \sim s^J$,[58,2] in which s is the square of the center-of-mass energy of final NN system ($s \approx (\frac{2}{x} - 1)Q^2 + 4m^2$). In the QCD description, in which hadrons are bound states of quarks and gluons, J is the Regge trajectory with quantum numbers permitted for a given process. Some trajectories are known experimentally: $J_\pi(t) \approx \alpha' t$, $J_\rho(t) \approx 0.5 + \alpha' t$, where $\alpha' \approx 1$ GeV^{-2} and t is the momentum transfer (see e.g. Ref. 59).

Since the transition in $A_{\Delta,N\to NN}$ is dominated by pion ($J = 0$) or ρ-type reggeon ($J = 1/2$) exchange the $\Delta N \to NN$ transition amplitude will be suppressed at least by a factor of $1/\sqrt{Q^2}$ compared to the elastic $NN \to NN$ amplitude. Thus, IC amplitude will be suppressed additionally at least by factor of $1/\sqrt{Q^2}$. This is the upper limit in the estimation of IC contribution, since the data on $NN \to N\Delta$ scattering indicate that the ρ regime is unimportant up to ISR energy ranges, thus in the Q^2 range of interest more rapid suppression is expected with the increase in Q^2.

It is interesting to note that the Q^2 dependence of electromagnetic form factors and the energy dependence of soft rescattering amplitudes of the other resonances (as N^*) are similar to the elastic form-factor of nucleon and NN soft rescattering amplitude (corresponding to the exchange of $J = 1$ reggeon), respectively. This fact which will be discussed later has an important implication in the emergence of the new regime, in which the quark-gluon degrees of freedom of the nucleons play an important role in hard exclusive nuclear reactions.

6. Final State Interactions

With an increase in energy, the characteristics of soft (small angle) hadron-hadron interactions in the amplitude of Fig. 2(b) simplify in several ways. The first major qualitative change is the emergence of a practically energy independent total cross-section of hadron-hadron interactions at lab momenta $\geq$ 1–1.5 GeV/c (total cross-sections are constant up to momenta of 400 GeV/c).

As Fig. 8 shows both *pp* and *pn* total cross-sections level out and become practically energy independent at lab momenta greater than a few GeV/c. This simplifies tremendously the description of the final state interactions since the small angle NN scattering is proportional to $\sigma_{NN}^{\text{total}}$. The additional simplification associated with the increase in energy is that at small angles the rescattering amplitude is predominately imaginary and conserves the helicity of interacting particles.

Finally, another consequence of high energy is the onset of a new (approximate) conservation law, which, as we will see later, has a significant impact in the analysis of semi-exclusive reactions.

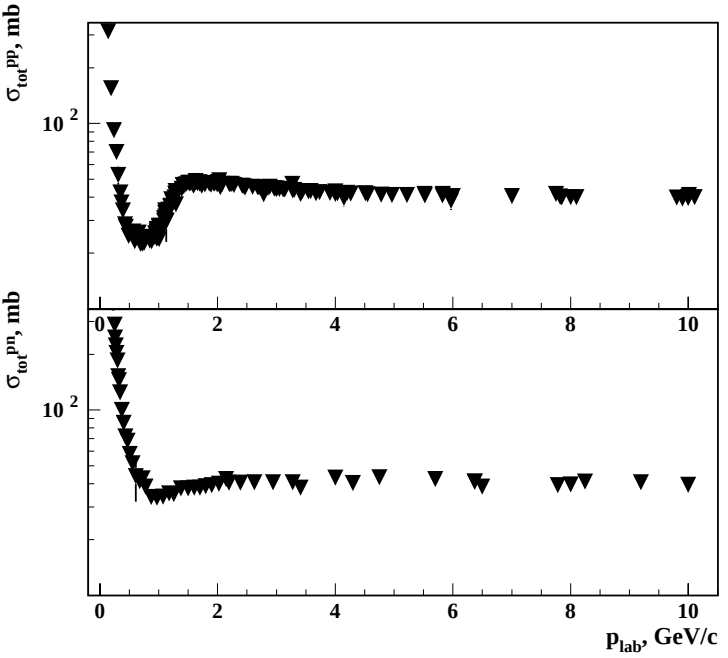

Fig. 8. Proton-proton and proton-neutron total cross-sections as a function of incoming proton momenta in lab. (Ref. 60).

6.1. *New (approximate) conservation rule*

In general, when a fast nucleon propagates through the nuclear medium it reinteracts with the target nucleons and, as a result, the information about the preexisting momentum distribution of the bound nucleons is distorted. Therefore, due to FSI the reconstructed missing momenta do not coincide with the actual momenta of the bound nucleon in the nucleus (for example $\mathbf{p}'_m \neq \mathbf{p}_m = \mathbf{p}_f - \mathbf{q}$ in Fig. 2(b)). Thus, FSI can severely hinder our ability to study the nuclear interior without disturbing it much. However, as we will see below, the increase in the energy of the propagating nucleon allows us to preserve some information about the momentum distribution of the bound nucleon.

Let us consider the propagation of a fast nucleon with four-momentum $k_1 = (\epsilon_1, k_{1z}, 0)$ through the nuclear medium. We choose the z axis in the direction of $\mathbf{k_1}$ such that $k_{1-}/m \approx m/2k_{1z} \ll 1$. After the small angle rescattering of this nucleon with the bound nucleon of four-momentum $p_1 = (E_1, p_{1z}, p_{1\perp})$, the energetic nucleon still attains its high momentum and leading z direction having now the four-momentum $k_2 = (\epsilon_2, k_{2z}, k_{2\perp})$ with $k_{2\perp}^2/m_N^2 \ll 1$ and the bound nucleon four-momentum becomes $p_2 = (E_2, p_{2z}, p_{2\perp})$. The energy momentum conservation for this scattering allows us to write for the "$-$" component:

$$k_{1-} + p_{1-} = k_{2-} + p_{2-}\,. \tag{17}$$

From Eq. (17) for the change of the "−" component of the bound nucleon momentum one obtains

$$\frac{\Delta p_-}{m} \equiv \frac{p_{2-} - p_{1-}}{m} \equiv \alpha_2 - \alpha_1 = \frac{k_{1-} - k_{2-}}{m} \ll 1\,, \tag{18}$$

where we define $\alpha_i = \frac{p_{i-}}{m}$, $i = 1, 2$ and use the fact that $k^2_{2\perp}/m^2_N$, $k^2_{1\perp}/m^2_N \ll 1$. Thus, Eq. 18 demonstrates that $\alpha_1 \approx \alpha_2$. The latter indicates that with the increase in energy a new conservation law emerges according to which the α of the bound nucleon is conserved. The uniqueness of the high energy rescattering is in the fact that although both energy and momentum of the bound nucleon are distorted due to rescattering, the combination of $E - p_z$ is not.

In Fig. 9 we demonstrate the accuracy of this conservation law for momenta of a propagating nucleon relevant for our considerations. It can be seen from Fig. 9 that the smaller the transferred momentum during rescattering, the better the accuracy of the conservation is. It is important to note that in the kinematic region given by Eq. (1) the average transfered momentum in the rescattering amplitude is $\langle k_t^2 \rangle \approx 0.250$ GeV$^2/c^2$, thus starting from 3–4 GeV/c momenta of the propagating nucleon the conservation of α ($\sim \mathcal{O}(1)$) is accurate to less than 5%.

The fact that information on the α distribution of the bound nucleons is preserved by FSI will play an important role in the investigation of short-range

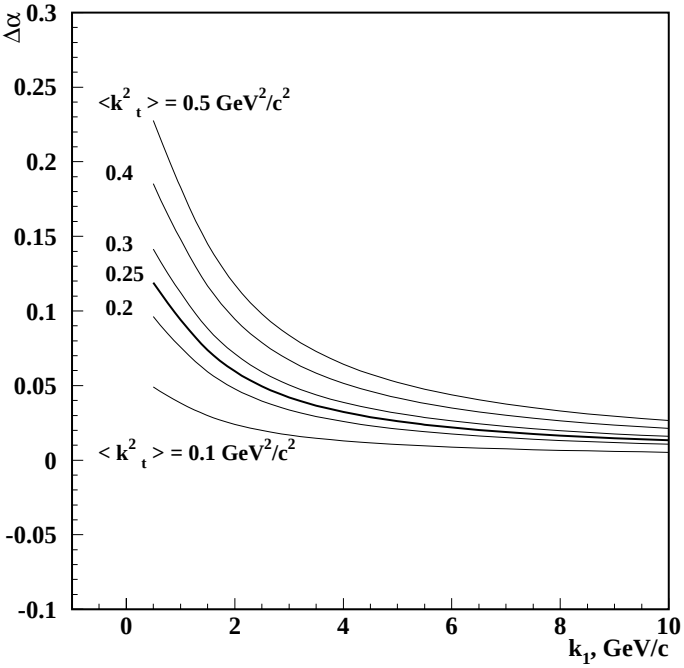

Fig. 9. The accuracy of the conservation of α as a function of the propagating nucleon momentum, k_1 at different values of average transferred (during the rescattering) momenta, $\langle k_t^2 \rangle$.

properties of nuclei in semi-exclusive reactions. Finally, it is worth mentioning that at small angles transferred momenta in the rescattering is practically transverse and its scattering amplitude can be parameterized as $f_{NN} \approx is\sigma_{\rm tot}e^{-\frac{B}{2}p_\perp^2}$.

6.2. *Reduction theorem*

Next, we will consider the following theorem: *High energy particles propagating in the nuclear medium cannot interact with the same bound nucleon a second time after interacting with another bound nucleon.* In other words, all those rescatterings which have segments similar to Fig. 10 are suppressed.

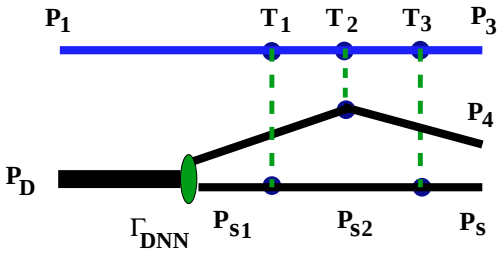

Fig. 10. Diagram for hadron-deuteron scattering.

We prove the above statement for the case of the amplitude of the diagram in Fig. 10. This proof can easily be generalized to all other cases. The invariant amplitude of the diagram in Fig. 10 can be presented as

$$A_{pd\to ppn} = -\int \frac{d^4p_{s1}}{i(2\pi)^4}\frac{d^4p_{s2}}{i(2\pi)^4}\frac{T_3(p_s-p_{s2})T_2(p_4-(p_D-p_{s1}))T_1(p_{s2}-p_{s1})}{D(p_3+p_s-p_{s2})D(p_1+p_{s1}-p_{s2})} \times \frac{\Gamma_{DNN}}{D(p_{s2})D(p_{s1})D(p_D-p_{s1})}\,, \tag{19}$$

where $D(p) = -(p^2-m^2+i\epsilon)$, and we neglect the spins since they are not relevant for our discussion.

The kinematics for the scattering corresponding to Fig. 10 is such that $p_{1+} \sim p_{3+} \gg m$ and $p_{1-} \sim p_{3-} \ll m$, i.e. the propagating nucleon at the top of Fig. 10 is very energetic, while $p_{4+} \sim p_{4-} \sim p_{s+} \sim p_{s-} \sim m$, i.e. the recoiled nuclear system is nonrelativistic.

Next, we introduce momenta:

$$k_1 = p_{s2}-p_{s1}\,, \qquad k_2 = p_s - p_{s2} \qquad \text{and} \qquad K = k_1+k_2\,. \tag{20}$$

Using these definitions and the relation $d^4K = \frac{1}{2}d^2K_\perp dK_- dK_+$ for Eq. (19) we obtain

$$A_{pd\to ppn} = \frac{1}{4}\int \frac{d^2K_\perp d^2k_{2\perp}}{(2\pi)^4}\frac{dK_- dk_{2-}}{(2\pi)^2}\frac{dK_+ dk_{2+}}{(2\pi)^2} \times \frac{T_3(k_2)T_2(p_4-(p_D-p_s+K))T_1(K-k_2)}{D(p_3+k_2)D(p_1+k_2-K)} \times \frac{\Gamma_{DNN}}{D(p_s-k_2)D(p_s-K)D(p_D-p_s+K)}\,. \tag{21}$$

First, we integrate over dK_+ and dk_{2+}. To do this we observe that only the poles in the denominators $D(p_s-k_2)$ and $D(p_s-K)$ give the finite contribution in the integral. Other poles in $D(p_3+k_2)$ and $D(p_1+k_2-K)$ correspond to the contribution at $|k_{2+}|\sim|p_{3+}|,|p_{1+}|\gg m$ and $K_+\sim p_{1+}\gg m$ and are strongly suppressed. Thus, one integrates over dK_+ and dk_{2+} by taking residues over the poles of the propagators $D(p_s-k_2)$ and $D(p_s-K)$ and obtains

$$A_{pd\to ppn} = \frac{-1}{4}\int \frac{d^2K_\perp d^2k_{2\perp}}{(2\pi)^4}\frac{dK_- dk_{2-}}{(2\pi)^2}\frac{T_3(k_2)T_2(p_4-(p_D-p_s+K))T_1(K-k_2)}{D(p_3+k_2)D(p_1+k_2-K)} \times \frac{\Gamma_{DNN}}{(p_s-k_2)_-(p_s-K)_- D(p_D-p_s+K)}\,. \tag{22}$$

Next, to integrate over dK_- and dk_{2-} one observes that in the high energy limit when $p_{1+},p_{3+}\gg m$ and $p_{1-},p_{3-}\ll m$ the fast nucleon's propagator can be expressed as

$$\begin{aligned} -D(p_3+k_2) &= (p_3+k_2)_+(p_3+k_2)_- - (p_3+k_3)^2_\perp - m^2 + i\epsilon \approx p_{3+}(k_{2-}+i\epsilon) \\ -D(p_1+k_2-K) &= (p_1+k_2-K)_+(p_1+k_2-K)_- - (p_1+k_2-K)^2_\perp - m^2 + i\epsilon \\ &\approx p_{1+}(k_{2-}-K_-+i\epsilon)\,. \end{aligned} \tag{23}$$

Inserting these expressions into Eq. (22) one obtains

$$A_{pd\to ppn} = \frac{-1}{4}\int \frac{d^2K_\perp d^2k_{2\perp}}{(2\pi)^4}\frac{dK_- dk_{2-}}{(2\pi)^2}\frac{T_3(k_2)T_2(p_4-(p_D-p_s+K))T_1(K-k_2)}{p_{3+}(k_{2-}+i\epsilon)p_{1+}(k_{2-}-K_-+i\epsilon)} \times \frac{\Gamma_{DNN}}{(p_s-k_2)_-(p_s-K)_- D(p_D-p_s+K)}\,. \tag{24}$$

Analyzing the range of the integration over dK_- and dk_{2-} we first observe that the soft rescattering amplitudes depend predominantly on $q_\perp$, i.e. $T_i(q)\sim T_i(q_\perp)$ and does not contain any singularities associated with K_- and k_{2-}. Other apparent singularities may come from $(p_s-k_2)_-=0$ and $(p_s-K)_-=0$. However, according to the redefinitions of Eq. (20) they correspond to $p_{s2-}=0$ and $p_{s1-}=0$. The latter conditions represent a bound nucleon with infinite virtuality $p_{s1+,2+}\sim m^2/p_{s1-,2-}$ which is suppressed by the wave function of bound nucleon. Therefore, the structure of dK_- and dk_{2-} integrations will be defined only by two denominators of a fast

propagating nucleon, i.e. by

$$\int \frac{dk_{2-}dK_-}{(k_{2-}+i\epsilon)(k_{2-}-K_-+i\epsilon)} = 0\,. \tag{25}$$

The above integral is zero since both poles over k_{2-} are on the same side of the complex k_{2-} semi-plane and one can close the contour of integration on the side where no singularities exist. Thus, this contribution results in $A_{pd\to ppn} = 0$.

This result allows us to reduce a potentially infinite number of rescattering diagrams to a finite set of diagrams. The only diagrams that survive are those in which a propagating fast nucleon interacts first with one target nucleon then the next one and so on, making rescatterings strictly sequential.

Another consequence of this theorem is that, if the virtuality of a bound nucleon, which is interacting with the propagating (energetic) nucleon, can be neglected, the sum of the interaction amplitudes with a given nucleon can be replaced by the invariant NN scattering amplitude, F_{NN} as in Fig. 11. The later can be replaced by the phenomenological NN scattering amplitude taken from the NN scattering data.

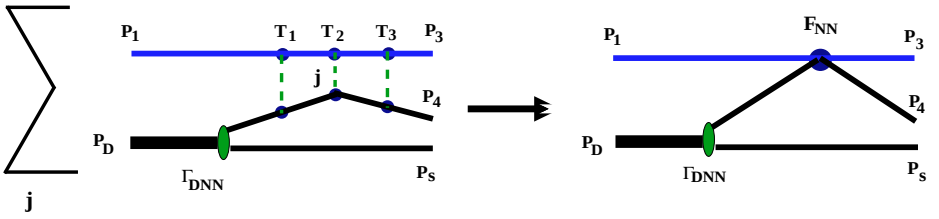

Fig. 11. The sum of the scattering vertices replaced by the NN scattering amplitude.

Thus, we will end up with the finite set of scattering diagrams for which Feynman diagram rules can be identified.

The above result represents the realization of eikonal approximation. However, the major difference from the conventional semiclassical approximation is that the present approach does not require the spectator nucleons to be a stationary scatterers.[19] Furthermore, we will refer to the present approach as generalized eikonal approximation (GEA).

7. Feynman Diagram Rules for the Scattering Amplitude in GEA

In this section we will define the effective Feynman diagram rules, within GEA, for the scattering amplitude of a knocked-out nucleon to undergo n rescatterings off the nucleons of the $(A-1)$ residual system. The case $n = 0$ corresponds to the plane wave impulse approximation in which the knocked out nucleon does not interact with the residual nucleus. We systematically neglect the diffractive excitation of the nucleons in the intermediate states. In soft QCD processes this is a small correction

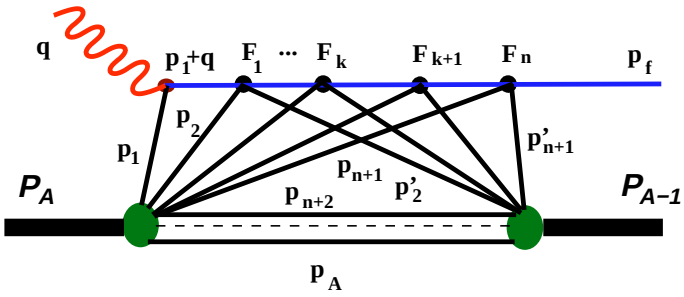

Fig. 12. Diagram for n-fold rescattering.

for the knock-out nucleon (projectile) energies $\lesssim$ 10 GeV. In the hard processes (that is, when Q^2, virtuality of the photon is sufficiently large ($\gtrsim$ 6–8 GeV^2)) such an approximation cannot be justified even within this energy range, because of the important role of quark-gluon degrees of freedom in Color Transparency phenomena (see for example the discussion in Ref. 39). However, our aim is to perform calculations in the kinematics where the color transparency phenomenon is still a small correction and intermediate hadronic states can be treated as nucleon states.

According to the above discussion the n-fold rescattering amplitude will be represented through n vertex amplitudes in which each vertex corresponds to one NN scattering — Fig. 12. We can formulate the following Feynman rules of calculation of the diagram in Fig. 12 (see also Ref. 62).

- We assign the vertex functions $\Gamma_A(p_1,\ldots,p_A)$ and $\Gamma^{\dagger}_{A-1}(p'_2,\ldots,p_A)$ to describe the transitions between "*nucleus A*" to "*A nucleons*" with momenta $\{p_n\}$, $\{p'_n\}$ and "$(A-1)$ *nucleons*" with momenta $\{p'_n\}$ to "$(A-1)$ *nucleon final states*," respectively.
- For the $\gamma^* N$ interaction, we assign vertex, $F_N^{em,\mu}$.
- For each NN interaction, we assign the vertex function $F_k^{NN}(p_{k+1},p'_{k+1})$. This vertex function is related to the amplitude of NN scattering as follows:

$$\bar{u}(p_3)\bar{u}(p_4)F^{NN}u(p_1)u(p_2)=\sqrt{s(s-4m^2)}f^{NN}(p_3,p_1)\delta_{\lambda,\lambda'}\approx sf^{NN}(p_3,p_1)\delta_{\lambda,\lambda'}\,, \tag{26}$$

where s is the total invariant energy of two interacting nucleons with momenta p_1 and p_2 and

$$f^{NN}=\sigma_{\rm tot}^{NN}(i+\alpha)e^{-\frac{B}{2}(p_3-p_1)_\perp^2}\,, \tag{27}$$

where $\sigma_{\rm tot}^{NN}$, α and B are known experimentally from NN scattering data. The vertex functions are accompanied with the δ-function of energy-momentum conservation.

- For each intermediate nucleon with four momentum p we assign propagator $D(p)^{-1}=-(\hat{p}-m+i\epsilon)^{-1}$. Following Ref. 50 we choose the "minus" sign for

the nucleon propagators to simplify the calculation of the overall sign of the scattering amplitude.

- The factor $n!(A-n-1)!$ accounts for the combinatorics of n-rescatterings and $(A-n-1)$ spectator nucleons.
- For each closed contour one gets the factor $1/i(2\pi)^4$ with no additional sign.

Using the rules defined above for the scattering amplitude of Fig. 12 one obtains

$$
\begin{aligned}
F^{(n)}_{A,A-1}(q,p_f) = \sum_h \frac{1}{n!(A-n-1)!} \prod_{i=1}^{A}\prod_{j=2}^{A} \int d^4p_i d^4p'_j \frac{1}{[i(2\pi)^4]^{A-2+n}} \\
\times \delta^4\left(\sum_{i=1}^{A} p_i - \mathcal{P}_A\right) \delta^4\left(\sum_{j=2}^{A} p'_j - \mathcal{P}_{A-1}\right) \prod_{m=n+2}^{A} \delta^4(p_m - p'_m) \\
\times \frac{\Gamma_A(p_1,\ldots,p_A)}{D(p_1)D(p_2)\cdots D(p_{n+1})D(p_{n+2})\cdots D(p_A)} \frac{F_N^{\rm em}(Q^2)}{D(p_1+q)} \\
\times \frac{f_1^{NN}(p_2,p'_2)\cdots f_n^{NN}(p_{n+2},p'_{n+2})}{D(l_1)\cdots D(l_k)\cdots D(l_{n-1})} \\
\times \frac{\Gamma_{A-1}(p'_2,\ldots,p'_{n+1},p_{n+2},\ldots,p_A)}{D(p'_2)\cdots D(p'_{n+1})}\,, \qquad (28)
\end{aligned}
$$

where, for the sake of simplicity, we neglect the spin dependent indices. Here $\mathcal{P}_A$ and $\mathcal{P}_{A-1}$ are the four momenta of the target nucleus and final $(A-1)$ system, respectively. p_j and p'_j are the nucleon momenta in the nucleus A and residual $(A-1)$ system, respectively. $\sum_h$ in Eq. (28) goes over virtual photon interactions with different nucleons, where $F_h^{\rm em}(Q^2)$ are electromagnetic vertices. $-D(p_k)^{-1}$ is the propagator of a nucleon with momentum p_k and $-D(l_k)^{-1}$ is the propagator of the struck nucleon in the intermediate state, with momentum $l_k = q+p_1+\sum_{i=2}^{k}(p_i-p'_i)$ between $(k-1)$th and kth rescatterings. The intermediate spectator states in the diagram of Fig. 12 are expressed in terms of nucleons, but not nuclear fragments because the closure over various nuclear excitations in the intermediate state is used. The possibility of using closure is related to the fact that the typical scale characteristic for high energy phenomena is significantly larger than the energy scale of nuclear excitations (for details see Appendix A).

After evaluation of the intermediate state nucleon propagators, the covariant amplitude will be reduced to a set of time-ordered noncovariant diagrams. This will help to establish the correspondence between the nuclear vertex functions and the nuclear wave functions. Particularly in the nonrelativistic limit the momentum space wave function is defined through the vertex function as[50,64]

$$
\psi_A(p_1,p_2,\ldots,p_A) = \frac{1}{\left(\sqrt{(2\pi)^3 2m}\right)^{A-1}} \frac{\Gamma_A(p_1,p_2,\ldots,p_A)}{D(p_1)}\,, \qquad (29)
$$

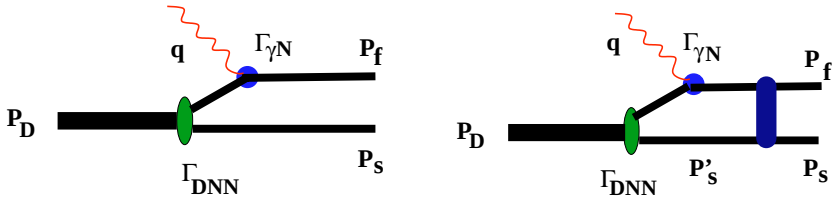

(a) (b)

Fig. 13. Diagrams for the $e + d \to e' + p + n$ reaction: (a) PWIA contribution, and (b) single rescattering contribution.

where wave functions are normalized as: $\int |\psi_A(p_1, p_2, \ldots, p_A)|^2 d^3p_1 d^2p_2 \cdots d^3p_A = 1$.

To demonstrate the application of the effective Feynman diagram rules we derive formulae for the impulse approximation and first two rescattering terms (i.e. single and double rescatterings). To simplify derivations, we consider $(e, e'N)$ reactions off the deuteron and $A = 3$ target (see Figs. 13, 19 and 20) and then generalize the obtained results for the case of large A.

8. Electro-disintegration of the Deuteron

To demonstrate the application of the effective Feynman rules in the calculation of the nuclear scattering amplitude, we first calculate the simplest case of electro-disintegration of the deuteron ($e + d \to e' + p + n$) in the kinematics of Eq. (1). We will apply the following restrictions on the momenta involved in the reaction:

$$Q^2 \geq 1 \text{ GeV}^2\,, \quad \mathbf{q} \approx \mathbf{p_f} \geq 1 \text{ GeV}/c \quad \text{and} \quad |\mathbf{p_s}| \leq 400 \text{ MeV}/c\,. \tag{30}$$

The last restriction allows us to neglect negative energy nucleon states (vacuum diagrams) and unambiguously identify the $D \to NN$ vertex multiplied by the propagator of the virtual nucleon with the nonrelativistic wave function of the deuteron. Thus, we will proceed with the calculation employing the approximation of $\mathcal{O}(p^2/m^2)$ in the calculation of virtuality of the interacting nucleon and only nucleon degrees of freedom will be taken into account. (The presence of negative energy states does not allow the above identification. The use of light-cone quantum mechanics helps to overcome this problem, but, as was mentioned in Sec. 4, the nuclear wave functions in this case are defined in the light-cone reference frame. However, in practice when the conditions of Eq. (30) are satisfied, all approaches should give rather similar results (see e.g. Ref. 61).)

8.1. *Plane wave impulse approximation*

The amplitude corresponding to the impulse approximation diagram of Fig. 13(a) can be written from Eq. (5):

$$A_0^\mu = -\frac{\bar{u}(p_s)\bar{u}(p_f)\Gamma^\mu_{\gamma^* N} \cdot [\hat{p}_D - \hat{p}_s + m] \cdot \Gamma_{DNN}}{(p_D - p_s)^2 - m^2 + i\epsilon}\,. \tag{31}$$

The kinematic restriction on p_s allows us to use approximation $\hat{p}_d - \hat{p}_s + m \approx \sum_\lambda u_\lambda(p_d - p_s)\bar{u}_\lambda(p_D - p_s)$ and introduce electromagnetic current for the bound nucleon as

$$j^\mu = \bar{u}(p_f)\Gamma^\mu_{\gamma^* N} u(p_D - p_s)\,. \tag{32}$$

Note that this current still has an ambiguity related to the off-shellness of the bound nucleon, however the effect is rather small for the kinematics of Eq. (30) (see e.g. Ref. 61). Using the definition of j^μ from Eq. (32) for the scattering amplitude, one obtains

$$A_0^\mu = -\frac{j^\mu \bar{u}(p_s)\bar{u}(p_D - p_s)\Gamma_{DNN}}{(p_D - p_s)^2 - m^2 + i\epsilon}\,. \tag{33}$$

Next, because one neglects negative energy contributions, we can identify the $D \to NN$ vertex with the nonrelativistic deuteron wave function as[50,63,64]

$$\frac{\bar{u}(p_s)\bar{u}(p_D - p_s)\Gamma_{DNN}}{[m^2 - (p_D - p_s)^2]\sqrt{(2\pi)^3 2m}} = \psi_D(p_s)\,. \tag{34}$$

It can be proven that the above defined wave function satisfies the nonrelativistic Schrödinger equation when the kinematic conditions given by Eq. (30) are valid. Inserting Eq. (34) into Eq. (33) for the scattering amplitude within IA one obtains

$$A_0^\mu = \sqrt{(2\pi)^3 2E_s}\psi_D(p_s) j^\mu(p_s, q)\,. \tag{35}$$

8.2. *Single rescattering amplitude*

To calculate the amplitude corresponding to the single rescattering — Fig. 13(b) — we apply the Feynman rules of Sec. 7 which results in

$$A_1^\mu = -\int \frac{d^4 p'_s}{i(2\pi)^4} \frac{\bar{u}(p_f)\bar{u}(p_s) F_{NN}[\hat{p}'_s + m][\hat{p}_D - \hat{p}'_s + \hat{q} + m]}{(p_D - p'_s + q)^2 - m^2 + i\epsilon}$$

$$\times \frac{\Gamma^\mu_{\gamma^* N}[\hat{p}_D - \hat{p}'_s + m]\Gamma_{DNN}}{((p_D - p'_s)^2 - m^2 + i\epsilon)(p'^2_s - m^2 + i\epsilon)}\,. \tag{36}$$

One can integrate the above equation over $d^0 p'_s$ observing that F_{NN} does not have a singularity in p'_s. It reflects the fact that at high energies, the total cross section of NN interaction depends only weakly on the collision energy (see e.g. Refs. 50 and 64).

The kinematic restrictions of Eqs. (1) and (30) (particularly $p_s \le 400$ MeV/c) allow us to evaluate the loop integral in Eq. (36) by taking the residue over the spectator nucleon energy in the intermediate state, i.e. we can replace $[p'^2_s - m^2 + i\epsilon]^{-1} d^0 p'_s$ by $-i(2\pi)/2E'_s \approx -i(2\pi)/2m$. This is possible because in this case it is the only pole in the lower part of the p'_{s0} complex plane. The calculation of the residue in p'_{s0} fixes the time ordering from left to right in Fig. 13(b). Since this integration puts the spectator nucleon in the intermediate state on its mass-shell, the Γ_{DNN} vertex with the interacting (with the photon) nucleon propagator will

have a similar construction as in the case of the IA diagram. Thus, using the relation of $\hat{p}_d - \hat{p}'_s + m \approx \sum_\lambda u_\lambda(p_d - p'_s)\bar{u}_\lambda(p_d - p'_s)$ and $\hat{p}'_s + m \approx \sum_\lambda u_\lambda(p'_s)\bar{u}_\lambda(p'_s)$ one can introduce the deuteron wave function according to Eq. (34). Furthermore, using Eqs. (26) and (32) we obtain

$$A_1^\mu = -\frac{(2\pi)^{\frac{3}{2}}\sqrt{2E_s}}{2m}\int \frac{d^3p'_s}{(2\pi)^3}\frac{sf_{pn}(p_{s\perp} - p'_{s\perp})}{(p_D - p'_s + q)^2 - m^2 + i\epsilon} \times j^\mu_{\gamma^* N}(p_D - p'_s + q, p_D - p'_s)\psi_D(p'_s)\,. \tag{37}$$

Now, we analyze the propagator of the knocked-out nucleon:

$$(p_D - p'_s + q)^2 - m^2 + i\epsilon = m_D^2 - 2p_D p'_s + p'^2_s + 2q(p_D - p'_s) - Q^2 - m^2 + i\epsilon\,. \tag{38}$$

We can simplify Eq. (38), using the relation of energy-momentum conservation:

$$(p_D - p_s + q)^2 = m^2 = m_D^2 - 2p_D p_s + m^2 + 2q(p_D - p_s) - Q^2\,, \tag{39}$$

which allows us to represent Eq. (38) as

$$(p_D - p'_s + q)^2 - m^2 + i\epsilon = 2|\mathbf{q}|\left[p'_{sz} - p_{sz} + \frac{q_0}{|\mathbf{q}|}(E_s - m) + \frac{m_D}{|\mathbf{q}|}(E_s - m) + \frac{p'^2_s - m^2}{2|\mathbf{q}|}\right]. \tag{40}$$

Keeping only the terms which do not vanish with increasing q (the first three terms in Eq. (40)) and observing that in the high energy limit (Eq. (3)) $2m|\mathbf{q}| \approx s$ for the scattering amplitude of Eq. (37), we obtain

$$A_1^\mu = -\frac{(2\pi)^{\frac{3}{2}}\sqrt{2E_s}}{2}\int \frac{d^3p'_s}{(2\pi)^3}\frac{f_{pn}(p_{s\perp} - p'_{s\perp})}{p'_{sz} - p_{sz} + \Delta + i\epsilon} j^\mu_{\gamma^* N}(p_D - p'_s + q, p_D - p'_s)\psi_D(p'_s)\,, \tag{41}$$

where

$$\Delta = \frac{q_0}{|\mathbf{q}|}(E_s - m)\,. \tag{42}$$

The fact that f_{pn} depends only weakly on the initial energy and is determined mainly by the transverse component of the transferred momentum helps us to carry out the integration over p'_{sz} in Eq. (41). For this, one uses the explicit form of the deuteron wave function as it is defined in the lab frame (see Eq. (B1)). Inserting Eq. (B1) into Eq. (41) one can analytically integrate over p'_{sz} (see Appendix B) arriving to the following expression for the single rescattering amplitude:

$$A_1^\mu = -\frac{(2\pi)^{\frac{3}{2}}\sqrt{2E_s}}{4i}\int \frac{d^2k_t}{(2\pi)^2} f_{pn}(k_t) j^\mu_{\gamma^* N}(p_D - \tilde{p}_s + q, p_D - \tilde{p}_s)[\psi_D(\tilde{p}_s) - i\psi'_D(\tilde{p}_s)]\,, \tag{43}$$

where we defined the transverse component of the momentum transfered during NN rescattering as $k_t = p'_{s\perp} - p_{s\perp}$. In Eq. (43), $\tilde{p}_s(\tilde{p}_{sz}, \tilde{p}_{s\perp}) \equiv \tilde{\mathbf{p}}_\mathbf{s}(p_{sz} - \Delta, p_{s\perp} - k_\perp)$, ψ_D

is the deuteron wave function defined in Eq. (B1) and ψ'_D is defined in Eqs. (B7) and (B8). Note that in general, $f_{pn}(k_t)$ which enters with ψ_D and $f_{pn}(k_t)$ that enters with ψ'_D are different, since in the latter case $f_{pn}(k_t)$ corresponds to the off-shell amplitude.[65] This off-shellness will most likely result in the reduction of the real part contribution. However, in many cases the overall contribution from ψ'_D is small and off-shell effects in $f_{pn}(k_t)$ can be neglected.

8.3. *Relation of GEA to the Glauber theory*

The next question we address is how the derivation of the rescattering amplitude discussed above is related to the Glauber theory. To make a pointed comparison we first factorize the electromagnetic current in Eq. (43) from the integral. (The validity of such factorization will be discussed in the next section.) Furthermore, it is convenient to perform integration of Eq. (41) in coordinate space. Writing the Fourier transform of the deuteron wave function as

$$\psi_D(p) = \frac{1}{(2\pi)^{\frac{3}{2}}} \int d^3r \phi_D(r) e^{-ipr}\,, \tag{44}$$

and using the coordinate space representation of the nucleon propagator

$$\frac{1}{[p'_{sz} - p_{sz} + \Delta + i\epsilon]} = -i \int dz^0 \Theta(z^0) e^{i(p'_{sz} - p_{sz} + \Delta)z^0}\,, \tag{45}$$

we obtain the folowing formula for the rescattering amplitude:

$$\begin{aligned} A_1^\mu &= -j^\mu(p_s + q, p_s) \frac{\sqrt{2E_s}}{2i} \int \frac{d^2k_\perp}{(2\pi)^2} d^3r \phi(r) f^{pn}(k_\perp) \theta(-z) e^{i(p_{sz} - \Delta)z} e^{i(p_{s\perp} - k_\perp)b} \\ &= -j^\mu(p_s + q, p_s) \frac{\sqrt{2E_s}}{2i} \int d^3r \phi(r) \theta(-z) \Gamma^{pn}(\Delta, -z, -b) e^{ip_s r}\,, \end{aligned} \tag{46}$$

where $\mathbf{r} = \mathbf{r}_p - \mathbf{r}_n$ and we defined a generalized profile function Γ as

$$\Gamma^{pn}(\Delta, z, b) = \frac{1}{2i} e^{-i\Delta z} \int f^{pn}(k_\perp) e^{-ik_\perp b} \frac{d^2k_\perp}{(2\pi)^2}\,. \tag{47}$$

One can see from Eq. (47) that Eq. (46) reduces to the Glauber approximation in the limit of zero longitudinal momentum transfer Δ. The dependence of the profile function on the longitudinal momentum transfer Δ originates from the nonzero momentum of the recoiled nucleon, p_s. (Glauber theory is derived in the approximation of stationary nucleons, i.e. for zero momenta of spectator nucleons in the target.) Even though this new factor in Eq. (42) could be small, it effects the cross-section due to the steep momentum dependence of the deuteron wave function (see the discussion in the next section). The same modified profile function, Eq. (47), is valid for the single rescattering amplitudes of any nucleus A.[62] Thus one can conclude that in the limit of single rescattering the generalization of Glauber approximation to the GEA is rather simple, it requires the adding of a phase factor — Δ in the

Glauber profile function — Eq. (47). Note that this result is analogous to the account for the finite coherence length effects in the vector meson production from nuclei in the eikonal approximation.[20]

8.4. *The cross section of deuteron electro-disintegration*

One can now calculate the cross-section of the deuteron electro-disintegration through the electron and deuteron electromagnetic tensors as

$$\frac{d\sigma}{dE'_e d\Omega'_e d^3p_f/2E_f d^3p_s/2E_s} = \frac{E'_e}{E_e}\frac{\alpha^2}{q^4}\eta_{\mu\nu}T_D^{\mu\nu}\delta^4(p_D + q - p_f - p_s)\,, \tag{48}$$

where $\eta_{\mu\nu} = \frac{1}{2}\,\mathrm{Tr}(\hat{k}_2\gamma_\mu\hat{k}_1\gamma_\nu)$. $k_1 \equiv (E_e, \mathbf{k}_1)$ and $k_2 \equiv (E'_e, \mathbf{k}_2)$ are the four-momenta of incident and scattered electrons, respectively. The electromagnetic tensor $T_D^{\mu\nu}$ of the deuteron is

$$T_D^{\mu\nu} = \sum_{\text{spin}} (A_0 + A_1)^\mu (A_0 + A_1)^\nu\,, \tag{49}$$

where A_0 and A_1 correspond to the impulse approximation and single rescattering amplitudes calculated in Secs. 8.1 and 8.2. For the numerical calculation, we apply the factorization approximation in calculating the rescattering amplitude of Eq. (43), namely, using the fact that in soft NN rescattering $\langle k_\perp^2\rangle_{\text{rms}} \sim 250\ \text{MeV}^2/c^2 \ll |\mathbf{q}|^2$ the bound nucleon electromagnetic current can be factorized out of the integral in Eq. (43). In this case one arrives at the distorted wave impulse approximation (DWIA) in which the scattering cross-section could be represented as a product of the off-shell eN scattering cross-section σ_{eN} and the distorted spectral function $S_D(p_f, p_s)$:

$$\frac{d\sigma}{dE'_e d\Omega'_e dp_f} = p_f^2 \sigma_{eN} S_D(p_f, p_s)\,. \tag{50}$$

The off-shell cross-section σ_{eN} contains ambiguity in the spinor part related to the fact that the knocked-out nucleon is bound (see e.g. Ref. 53). However, the restrictions of Eq. (30) keep these ambiguities for the $q \sim$ a few GeV/c region reasonably small (see Ref. 61).

The distorted spectral function can be represented as

$$S(p_f, p_s) = \left|\psi_D(p_s) - \frac{1}{4i}\int \frac{d^2k_t}{(2\pi)^2} f_{pn}(k_t)\cdot[\psi_D(\tilde{p}_s) - i\psi'_D(\tilde{p}_s)]\right|^2\,. \tag{51}$$

To analyze the effects of rescattering in the cross-section, we calculate the ratio of the cross-section of Eq. (50) to the cross-section calculated within the plane wave impulse approximation, in which only the IA amplitude A_0 is included:

$$T = \frac{\sigma^{\text{IA+FSI}}}{\sigma^{\text{IA}}} = \frac{S(p_f, p_s)}{|\psi_D(p_s)|^2}\,. \tag{52}$$

Figure 14 demonstrates the calculation of T as a function of the recoil nucleon angle θ_{sq} with respect to $\mathbf{q}$ for different values of recoil nucleon momentum.

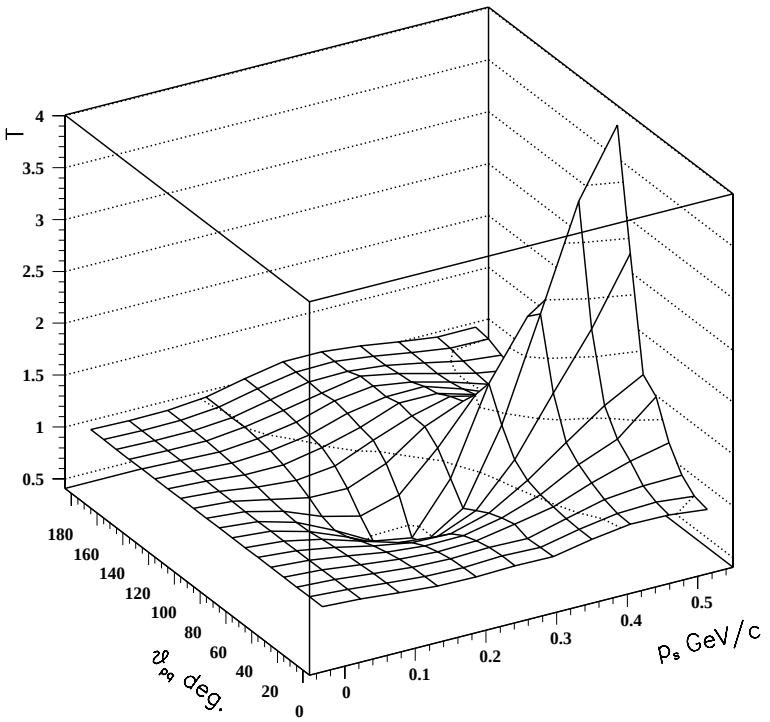

Fig. 14. The dependence of the transparency T on the angle, θ_{sq} and the momentum, p_s of the recoil nucleon. The angle is defined with respect to the $\mathbf{q}$.

Figure 14 demonstrates the distinctive angular dependence of ratio T. At recoil nucleon momenta $p_s \leq 300$ MeV/c, T has a minimum, and generally $T < 1$ while at $p_s > 300$ MeV/c, $T > 1$ and has a distinctive maximum.

One can easily understand the structure of T by recalling that the soft rescattering amplitude is mainly imaginary $f_{pn} = \sigma_{\rm tot}(i+\alpha)e^{-\frac{B}{2}k_\perp^2}$ with $\alpha \ll 1$. In this case inserting Eq. (51) into Eq. (52) for T one obtains

$$T \approx 1 - \frac{1}{2}\left|\frac{\psi_D(p_s)\int \frac{d^2k_\perp}{(2\pi)^2} f_{pn}(k_\perp)[\psi_D(\tilde{p}_s) - i\psi'_D(\tilde{p}_s)]}{\psi_D^2(p_s)}\right| + \frac{1}{4}\frac{\left|\int d^2k_\perp (2\pi)^2 f_{pn}(k_\perp)[\psi_D(\tilde{p}_s) - i\psi'_D(\tilde{p}_s)]\right|^2}{\psi_D^2(p_s)}\,. \tag{53}$$

From Eq. (53) one observes that the interference term has a negative sign and is proportional to $\psi_d(p_{sz}, p_{s\perp})\psi_d(p_{sz} - \Delta, p_{s\perp} - k_\perp)/\psi_d^2(p_{sz}, p_{s\perp})$. Thus, in the kinematics when the interference term is dominant the pn rescattering results in the screening of the overall cross-section, and thus $T < 1$. The maximal screening is found at $p_{st} \approx 200$ MeV/c at which the square of the rescattering term (the third term in Eq. (53)) is small and $T \leq 1$. Further increase in p_s suppresses the

relative contribution of the interference term compared to the square of rescattering term which results in $T > 1$. The dominance of the rescattering term compared to the interference term, with increasing p_s, can be understood from the fact that the interference term grows as $\sim 1/|\psi_D(p_s)|$ while the rescattering term grows as $\sim 1/|\psi_D(p_s)|^2$.

8.5. *Once more about the relation of GEA to the Glauber theory*

It is very illustrative to compare the predictions for T calculated within GEA and the Glauber approximation.

As Fig. 15 demonstrates, the predictions based on GEA are rather close to that for the Glauber approximation when recoil nucleon momentum is small. (Recall that Glauber theory is derived for the cases when the target nucleons are considered as stationary scatterers and therefore their Fermi momenta have been neglected.) However, at larger Fermi momenta predictions of both approaches differ considerably. For example for $p_s = 400$ MeV/c the GEA and the Glauber approximation predictions for angular dependence of the maximal contribution of the rescattering amplitude (i.e. the position of the maximum of T in Fig. 15) differ by as much as 30°. Such a difference is quite dramatic and can be checked in the forthcoming experiments at Jefferson Laboratory.[66–69]

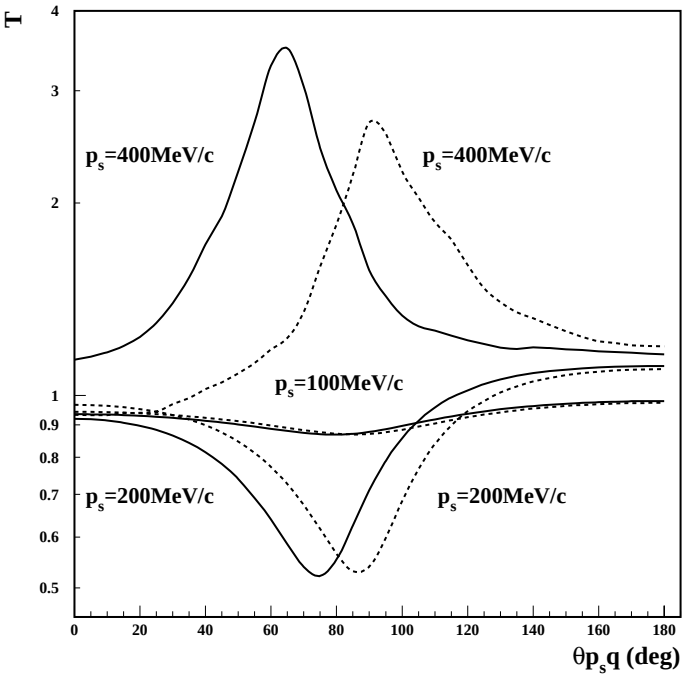

Fig. 15. The $\theta_{p_s q}$ dependence of T at different values of p_s. (Solid lines: GEA, dashed lines: Glauber approximation.)

8.6. *The Q^2 dependence of T and phenomenon of color coherence*

So far we have discussed only the p_s and $\theta_{p_s q}$ dependence of T. However, another interesting feature of T is its Q^2 dependence. As was discussed previously, one of the important features of high energy scattering is the energy independence of the NN soft scattering cross-section (e.g. Fig. 8), which enters into the rescattering amplitude (Fig. 13(b)) of the $d(e, e'N)N$ reaction. According to Eqs. (30) and (27) such energy independence should be reflected in the Q^2 independence of T (Eq. (53)) at fixed values of recoil nucleon momenta. As Fig. 16 shows indeed with increasing Q^2, T becomes practically Q^2 independent at a given value of p_s.

The Q^2 independence of T within GEA can be used as a baseline reference point to study the onset of the color coherence regime in high Q^2 exclusive reactions off nuclei. The idea of this phenomenon is based on the observation that at high $Q^2 \geq Q_0^2$ ($Q_0^2 \approx$ 6–8 GeV^2) the elastic $\gamma^* - N$ interaction is dominated by the contribution of the minimal Fock component of the quark-gluon wave function of the nucleon. The minimal Fock component of the hadronic wave function corresponds to the small sized, point-like configurations (PLC) in the hadrons. Thus, at $Q^2 \geq Q_0^2$ in the QCD picture one expects that hard elastic scattering will select the PLC from the wave function of the nucleon. Note that this feature is characteristic of both the perturbative[70,71] and nonperturbative[72] regime of QCD. If PLC are indeed

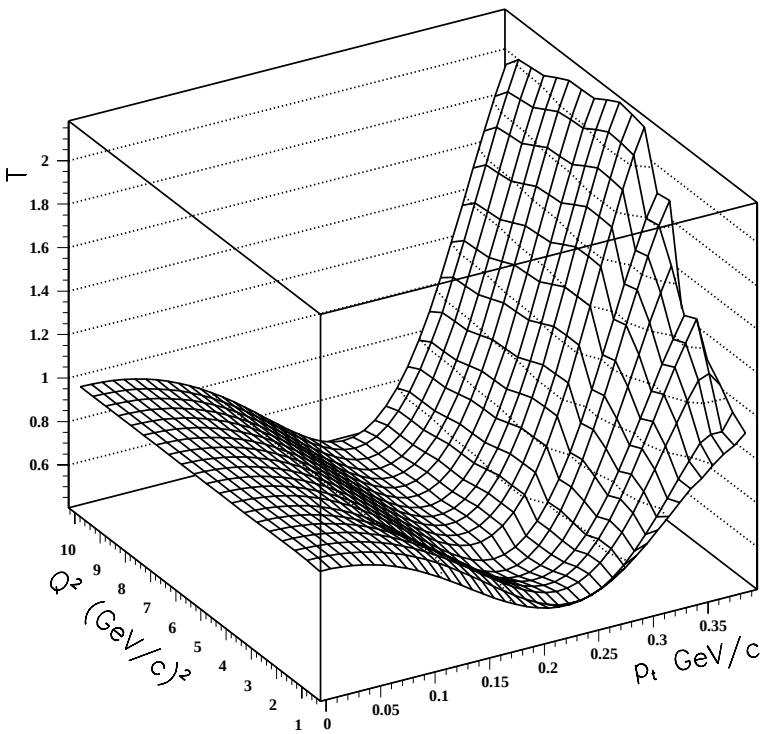

Fig. 16. T as a function of Q^2 and p_{st} at $\alpha_s = \frac{E_s - p_{sz}}{m} = 1$.

produced in high Q^2 exclusive reactions then, because of color screening (PLC are color singlet objects), one expects that they should propagate through the nuclear medium without final state interactions[73,74] — a phenomenon called Color Transparency (CT) (for reviews see Refs. 39 and 75). This phenomenon is observed at FNAL in the high energy regime when perturbative QCD is valid (see Refs. 76–78 and references therein).

However, in the nonperturbative QCD domain, observation of color coherence phenomena is complicated by the fact that at finite energies PLC will evolve to the normal hadronic state during its propagation through the nucleus.

As a result FSI will not be negligible at the later stages of the interaction. It is believed that the expansion of PLC was the major reason that prevented the observation of the onset of color coherence in $A(e,e'p)X$ reactions in the range of $Q^2 \sim 8$ GeV^2.[6,9] Thus, the major issue in the studies of color coherence phenomena in the nonperturbative regime is the suppression of the expansion of PLC. As was shown in Refs. 61 and 79 such a suppression can be achieved in exclusive $d(e,e'N)N$ reactions in which the selection of larger values of $p_{s\perp}$ allows the suppression of the distance between the space-time point of $\gamma^* N$ interaction and $PLC-N$ reinteraction. As a result, one can suppress the expected effects of a PLC expansion considerably.

There are several nonperturbative models which allow an estimation of the expected effects of color coherence incorporating a PLC expansion (see e.g. Refs. 80–85). To illustrate the expected magnitude of the phenomenon, we use the Quantum Diffusion Model (QDM) of Ref. 80. In the QDM the reduced interaction between the PLC and the spectator neutron (to be specific, we use a neutron as a spectator) can be accounted for by introducing the dependence of the scattering amplitude on the transverse size of the PLC. However, since we consider energies that are far from asymptotic, the expansion of PLC should be important. This feature is included by allowing the rescattering amplitude to depend on the distance from the photon absorption point. Within QDM for PLC-N scattering amplitudes one obtains[61,80]:

$$f^{\mathrm{PLC},N}(z,k_t,Q^2) = i\sigma_{\mathrm{tot}}(z,Q^2)e^{\frac{b}{2}t}\frac{G_N(t\sigma_{\mathrm{tot}}(z,Q^2)/\sigma_{\mathrm{tot}})}{G_N(t)}\,, \tag{54}$$

where $b/2$ is the slope of elastic NN amplitude, $G_N(t)$ ($\approx (1-t/0.71)^2$) is the Sachs form factor and $t=-k_t^2$. The last factor in Eq. (54) accounts for the difference between the elastic scattering of PLC and average configurations, using the observation that the t dependence of $d\sigma^{h+N\to h+N}/dt$ is roughly that of $\sim G_h^2(t)G_N^2(t)$ for not very large values of t and that $G_h^2(t) \approx \exp(R_h^2 t/3)$.

In Eq. (54) $\sigma_{\mathrm{tot}}(l,Q^2)$ is the effective total cross-section of the interaction of the PLC at distance l from the interaction point. The quantum diffusion model[80] corresponds to

$$\sigma_{\mathrm{tot}}(l,Q^2) = \sigma_{\mathrm{tot}}\left\{\left(\frac{l}{l_h}+\frac{\langle r_t(Q^2)^2\rangle}{\langle r_t^2\rangle}\left(1-\frac{l}{l_h}\right)\right)\Theta(l_h-l)+\Theta(l-l_h)\right\}\,, \tag{55}$$

where $l_h = 2p_f/\Delta M^2$, with $\Delta M^2 = 0.7$–1.1 GeV^2. Here $\langle r_t(Q^2)^2\rangle$ is the average transverse size squared of the configuration produced at the interaction point. In several realistic models considered in Ref. 86 it can be approximated as $\langle r_t(Q^2)^2\rangle/\langle r_t^2\rangle \sim 1\,\text{GeV}^2/Q^2$ for $Q^2 \geq 1.5$ GeV^2. Note that due to the effects of expansion, the results of calculations are rather insensitive to the value of this ratio whenever it is much less than unity. The calculation of the deuteron electrodisintegration cross-section within the QDM is performed by rewriting the amplitude of Eq. (43) in coordinate representation and using $f^{\text{PLC},N}$ from Eq. (54) to replace the amplitude of NN scattering, f_{pn}.

Other nonperturbative models which incorporate both the production of PLC and its expansion during the propagation are based on the observation that with an increase in energies the contribution from the inelastic transitions with intermediate baryonic resonances of the same spin as the nucleon (as N^* and N^{**}) are not further suppressed. As a result one expects that the intermediate hadronic state (after the γ^*N vertex in the diagram of Fig. 13(b)) to represent the superposition of the nucleonic, baryonic excitation and continuum states. The requirement that at high Q^2 γ^*N produces a PLC imposes additional constraints on the structure of this intermediate state.

In practical calculations the intermediate state is modeled through the two or three resonance states.[81,82,84,85] The three-state model is based on the assumption that the hard γ^*N scattering operator produces a non-interacting PLC which is a superposition of three baryonic states[82]:

$$|\text{PLC}\rangle = \sum_{m=N,N^*,N^{**}} F_{m,N}(Q^2)|m\rangle\,, \tag{56}$$

where $F_{m,N}(Q^2)$ are elastic ($m = N$) and inelastic transition form factors. The noninteraction of the initially produced PLC is provided by the condition: $T_S|\text{PLC}\rangle = 0$, where T_S is the 3×3 Hermitian matrix representing the small angle final state interactions. The relevant cross-section is obtained from Eq. (54), replacing f_{pn} by T_S. The detailed numerical calculations done in Ref. 61 demonstrate that both QDM and resonance models predict similar magnitudes for the effect of the suppression of final state rescatterings. Thus, in further estimations we will be restricted by QDM calculations only.

To be able to register the signature of the color coherence effect, it is important to identify the quantity which is most sensitive to the suppression of FSI with increasing Q^2. As can be seen from Fig. 14, within GEA the FSI is dominant in the transverse kinematics $\theta_{p_sq} \approx 90^\circ$ (more precisely when $\alpha_s = (E_s - p_{sz})/m = 1$). Besides, as follows from Figs. 14 and 15 at $p_s \lesssim 300$ MeV/c FSI dominates in the interference term of Eq. (53) thus the screening term is dominant and $T < 1$. At $p_s \gtrsim 350$ MeV/c the dominant contributions arise from the double scattering term in Eq. (53) and as a result $T > 1$. This observation allows us to define the ratio of the cross-section, measured at kinematics where double scattering is dominant, to the cross-section measured at kinematics where the effect of the screening is more important.

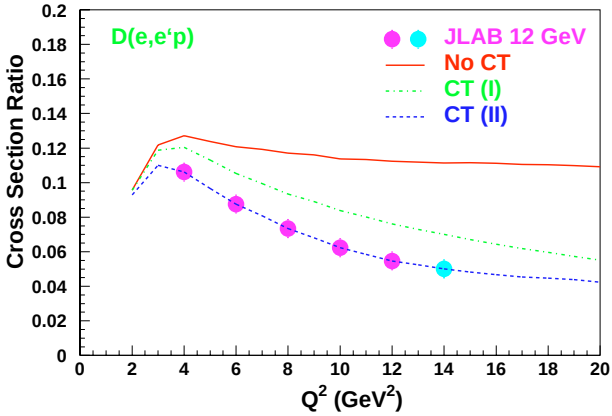

Fig. 17. The Q^2 dependence of the ratio R as defined in Eq. (57) for the reaction $d(e,e'p)n$ reaction. The solid curve is a generalized eikonal approximation. Dashed and dash-dotted curves correspond to the prediction of the quantum diffusion model with $\Delta M = 0.7$ GeV^2 (maximal CT) and $\Delta M = 1.1$ GeV^2 (minimal CT), respectively. The full circles are the projected data for 12 GeV upgrade of JLAB.[14]

Figures 14 and 15 show that it is possible to separate these two kinematic regions by choosing two momentum intervals for the recoil nucleon; (350–500 MeV/c) for double scattering and (0–250 MeV/c) for the screening. Thus, the suggested experiment will measure the Q^2 dependence of the following typical ratio:

$$R = \frac{\sigma(p = 400 \text{ MeV}/c)}{\sigma(p = 200 \text{ MeV}/c)}. \tag{57}$$

As Fig. 17 demonstrates the onset of color transparency will result in the decrease in the ratio R with increasing of Q^2, while GEA predicts practically no Q^2 dependence starting at $Q^2 \geq 4$ GeV^2. The circles in Fig. 17 correspond to the experimental data projected for the 12 GeV upgrade of CEBAF at Jefferson Lab.[14] Note that, in addition to the $d(e,e'pn)$ process, one can consider the excitation of baryon resonances with spectator kinematics, like $D(e,e'pN^*)$ and $D(e,e'N\Delta)$. The latter process is of special interest for looking for the so-called chiral transparency, the disappearance of the pion field of the ejectile.[79,87]

8.7. *Relation to the calculations based on intermediate energy approaches*

For completeness of the discussion on electro-disintegration of the deuteron, we address the question of overlap and continuity between the predictions of the approaches of intermediate and high energy physics.

In practice, the important question is whether the predictions of intermediate and high energy theories match at borderline kinematics. For borderline kinematics we consider the electro-disintegration of the deuteron at $Q^2 = 1$ GeV^2 with all other kinematical constraints defined in Eq. (30). In Fig. 18 we compare the prediction

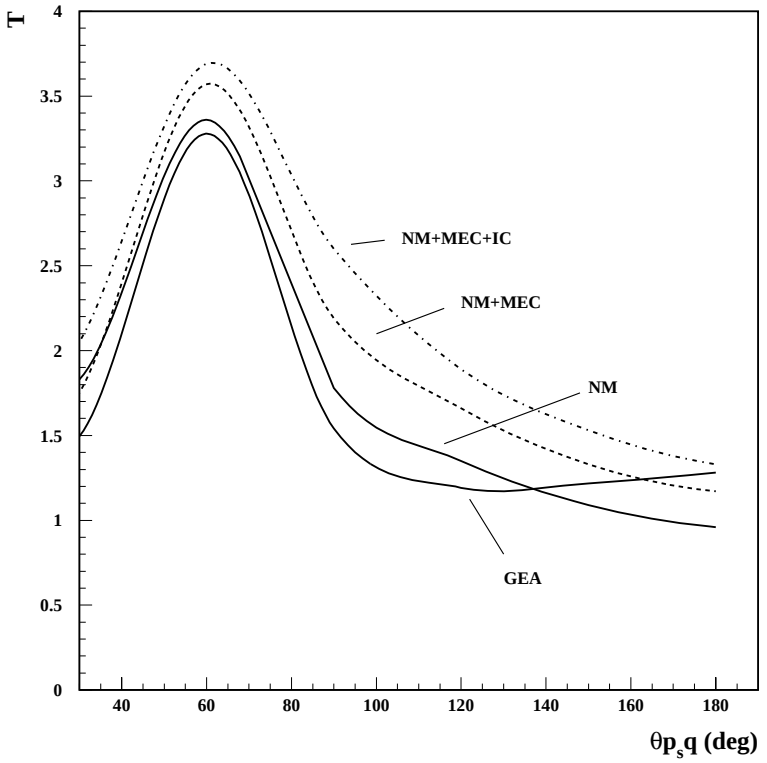

Fig. 18. The θ_n dependence of ratio T at $Q^2 = 1$ GeV^2. The curve marked "NM" corresponds to the cross section including final state interactions calculated in Ref. 44. The curves with "NM+MEC" and "NM+MEC+IC" correspond to the calculations of Ref. 44 including meson exchange currents and Isobar contributions, respectively.

of GEA with the results of calculations of the model of Ref. 44. Here $Q^2 = 1$ GeV^2 can be considered as an upper limit for the model of Ref. 44, in which up to seven orbital moments are included to account for the final state reinteraction. On the other hand $Q^2 = 1$ GeV^2 corresponds to the lower limit of validity of the GEA since the kinematical constraints of Eq. (3) are barely satisfied. As Fig. 18 shows one has surprisingly good agreement between the GEA and the model of Ref. 44 when no MEC and IC contributions are included. As we discussed above, with increasing Q^2 the relative contribution of MEC and IC should decrease, when compared with IA and FSI. This demonstrates the existence of continuity between both methods of calculation.

9. Electro-disintegration of Nuclei with $A \geq 3$

We now consider the electro-disintegration of nuclei with $A \geq 3$ (Fig. 19). The impulse approximation and single rescattering contribution can be generalized from Eqs. (35) and (41), respectively.

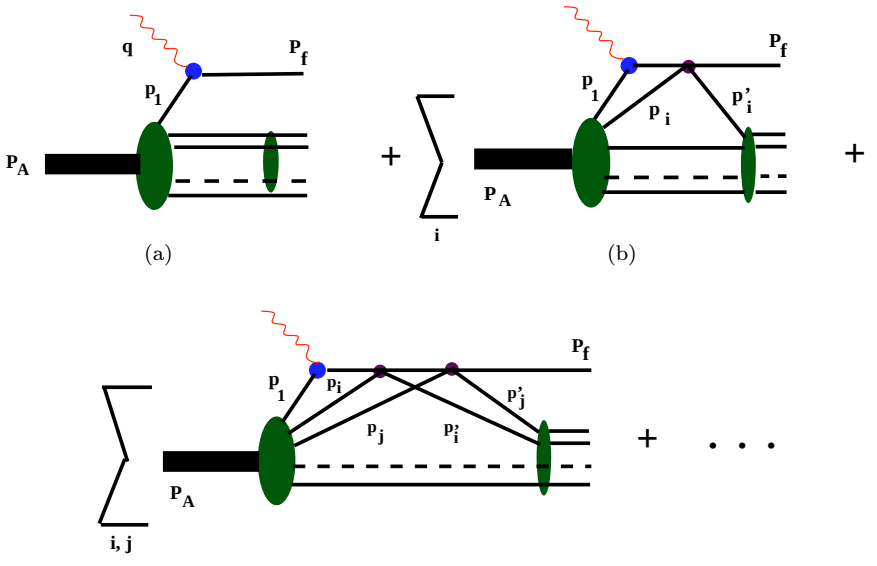

Fig. 19. Diagrams of $A(e,e'N)X$ reactions. (a) PWIA term, (b) single rescattering term, and (c) double rescattering term, and so on.

9.1. *Impulse approximation*

For the IA term one obtains

$$A_0^\mu = F \int \Psi^+_{A-1}(p_2,p_3,\ldots,p_A) j^\mu(p_m,q) \Psi_A(p_m,p_2,p_3,\ldots,p_A) d^3p_2 d^3p_3 \cdots d^3p_A \,, \tag{58}$$

where $\mathbf{p_m} = \mathbf{p_f} - \mathbf{q}$ and F is the phase space factor for the residual $A-1$ nuclear system. For example, for two-body break-up reactions $F = \sqrt{(2\pi)^3 2E_{A-1}}$ or for three-body break-up reactions on an $A=3$ target $F = \sqrt{(2\pi)^3 2E_{s1}(2\pi)^3 2E_{s2}}$ in which E_{s1} and E_{s2} are the energies of the two recoil nucleons.

9.2. *Single rescattering contribution*

For the single rescattering term (Fig. 19(b)) we generalize Eq. (41) to obtain

$$A_1^\mu = -\frac{F}{2} \sum_{i=2,A} \int \Psi^+_{A-1}(p_2,p'_i,\ldots,p_A) \frac{f_{NN}((p'_i - p_i)_\perp)}{p_{mz} - p_{1z} + \Delta + i\epsilon}$$

$$\times j^\mu(p_1,q) \Psi_A(p_1,p_2,p_i,\ldots,p_A) \frac{d^3p_1}{(2\pi)^3} d^3p_2,\ldots' \ldots d^3p_A \,, \tag{59}$$

where "$'$" in the integration means it does not contain p_i. From energy-momentum conservation one has $p_1 = \mathcal{P}_A - p_i - p_2 - p_A$ and $p'_i = \mathcal{P}_{A-1} - p_2 - \ldots' \ldots p_A$, where "$'$" means the exclusion of the ith nucleon's momentum.

If we transform the integrations into coordinate space, one can easily see that the only difference from the Glauber theory is the modification of the profile function according to Eq. (47). Therefore, the relation between the GEA and the Glauber theory in the limit of single rescatterings is rather straightforward and the only modification required is the phase factor in Eq. (47). Note that the Δ factor depends on the particular reactions. For example, in the case of a two-body break-up:

$$\Delta = \frac{q_0}{|\mathbf{q}|}\frac{p_m^2}{2M_{A-1}} + |\epsilon_b|\,, \tag{60}$$

where ϵ_b is the nuclear binding energy. For this relation one can see that for the case of large A, $\Delta \sim 0$ for large values of p_m. Therefore, one can conclude that the Glauber theory can be extended to the region of large values of missing-momenta p_m for two-body break-up reactions with large A nuclei.[38] For the case of three-body break-up of a $A = 3$ target:

$$\Delta = \frac{q_0}{|\mathbf{q}|}(T_{s1} + T_{s2} + |\epsilon|)\,, \tag{61}$$

where T_{s1} and T_{s2} are the kinetic energies of the two recoil nucleons in the reaction, and it cannot be neglected in the processes with large values of missing momentum p_m.

9.3. *Double rescattering contribution*

For the double rescattering contribution we have to calculate the two diagrams of Fig. 20. Using the Feynman diagram rules from Sec. 7 for the amplitudes of Fig. 20(a) one obtains:

$$\begin{aligned} A^{\mu}_{2a} = &\int \frac{\Gamma^+(p_2',p_3')}{D(p_2')D(p_3')}\frac{F^{NN}(p_3'-p_3)}{D(p_1+q+p_2-p_2')}\frac{F^{NN}(p_2'-p_2)}{D(p_1+q)}j^{\mu}(p_1,q)\frac{\Gamma(p_1,p_2,p_3)}{D(p_1)D(p_2)D(p_3)} \\ &\times \delta^4(p_A-p_2-p_3-p_1)\delta^4(p_{A-1}-p_2'-p_3')d^4p_1d^4p_2d^4p_3d^4p_2'd^4p_3'\left[\frac{1}{i(2\pi)^4}\right]^3 \\ = &\int \frac{\Gamma^+(p_2',p_3')}{D(p_2')D(p_3')}\frac{f^{NN}(p_3'-p_3)}{D(p_1+q+p_2-p_2')}\frac{f^{NN}(p_2'-p_2)}{D(p_1+q)} \\ &\times j^{\mu}(p_1,q)\frac{\Gamma(p_1,p_2,p_3)}{D(p_1)D(p_2)D(p_3)}\frac{d^4p_2}{i(2\pi)^4}\frac{d^4p_3}{i(2\pi)^4}\frac{d^4p_3'}{i(2\pi)^4}\,, \end{aligned} \tag{62}$$

where

$$p_1 = \mathcal{P}_A - p_3 - p_2 \quad \text{and} \quad p_2' = \mathcal{P}_{A-1} - p_3'\,. \tag{63}$$

Here again for simplicity we are neglecting the spins. Then, using the same approximations as for the cases of IA and single rescattering amplitudes, we can perform integration over d^0p_2, d^0p_3 and d^0p_3', which effectively results in the replacement $\int \frac{d^0p_j}{2\pi i D(p_j)} \to \frac{1}{2E_j} \approx \frac{1}{2m}$, $(j = 2, 3, 3')$.

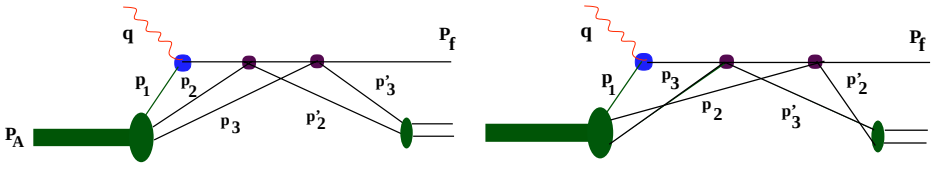

Fig. 20. Double rescattering diagram for the $^3\mathrm{He}(e,e'N)X$ reaction.

Using Eq. (63) and the definition of the initial and final state wave functions from the relations analogous to the Eq. (34) we obtain

$$A^{\mu}_{2a} = \frac{F}{4m^2}\int \psi^{+}_{A-1}(p'_2,p'_3)\frac{F^{NN}(p'_3-p_3)}{D(p_1+q+p_2-p'_2)}\frac{F^{NN}(p'_2-p_2)}{D(p_1+q)}$$
$$\times j^{\mu}(p_1,q)\psi_A(p_1,p_2,p_3)\frac{d^3p_1}{(2\pi)^3}\frac{d^3p_3}{(2\pi)^3}\frac{d^3p'_3}{(2\pi)^3}\,, \tag{64}$$

where $D(p_1+q)$ is the same as for the case of single rescattering. In the high energy limit:

$$-D(p_1+q) \approx 2|\mathbf{q}|(p_{zm}-p_{1z}+\Delta+i\epsilon)\,, \tag{65}$$

where Δ is defined by Eq. (60) or (61). For $D(p_1+q+p_2-p'_2)$, using Eq. (63) we obtain

$$\begin{aligned}-D(p_1+q+p_2-p'_2) &= -D(q+p_A-p_{A-1}+p'_3-p_3)\\ &= (q+p_A-p_{A-1}+p'_3-p_3)^2-m^2+i\epsilon\\ &\approx 2q\left[\frac{q_0}{q}(E'_3-E_3)-(p'_{3z}-p_{3z})+i\epsilon\right]\\ &= [(\Delta_3-(p'_{3z}-p_{3z})+i\epsilon]\,.\end{aligned} \tag{66}$$

In the derivation of Eq. (66) we use the kinematic condition for the quasielastic scattering: $(q+p_A-p_{A-1})^2=m^2$ and define $\Delta_3=\frac{q_0}{q}(E'_3-E_3)$. Similar to the single rescattering case, introducing f_{NN} amplitudes, one obtains

$$A^{\mu}_{2a} = \frac{F}{4}\int \psi^{+}_{A-1}(p'_2,p'_3)\frac{f^{NN}(p'_3-p_3)}{\Delta_3-(p'_{3z}-p_{3z})+i\epsilon}\frac{f^{NN}(p'_2-p_2)}{p^m_z+\Delta-p_{1z}+i\epsilon}$$
$$\times j^{\mu}(p_1,q)\psi_A(p_1,p_2,p_3)\frac{d^3p_1}{(2\pi)^3}\frac{d^3p_3}{(2\pi)^3}\frac{d^3p'_3}{(2\pi)^3}\,. \tag{67}$$

To complete the calculation of double scattering amplitude, one should also calculate the amplitude corresponding to the diagram of Fig. 20(b). This amplitude can be obtained by interchanging the momenta of nucleon "2" and "3." Doing so, for

the complete double scattering amplitude, one obtains

$$A_2^\mu = A_{2a}^\mu + A_{2b}^\mu = \frac{F}{4}\int \psi^+_{A-1}(p'_2,p'_3) \times \left[\frac{f^{NN}(p'_3-p_3)}{\Delta_3-(p'_{3z}-p_{3z})+i\epsilon}\frac{f^{NN}(p'_2-p_2)}{p_z^m+\Delta-p_{1z}+i\epsilon} + \frac{f^{NN}(p'_2-p_2)}{\Delta_2-(p'_{2z}-p_{2z})+i\epsilon}\frac{f^{NN}(p'_3-p_3)}{p_z^m+\Delta-p_{1z}+i\epsilon}\right] \times j^\mu(p_1,q)\psi_A(p_1,p_2,p_3)\frac{d^3p_1}{(2\pi)^3}\frac{d^3p_3}{(2\pi)^3}\frac{d^3p'_3}{(2\pi)^3}\,, \tag{68}$$

where $\Delta_2 = \frac{q_0}{q}(E'_2 - E_2)$. Similar to the case of single rescattering, one can now generalize Eq. (68) for the case of $A > 3$, which will read

$$A_2^\mu = \frac{F}{4}\sum_{i\neq j=2}^{A}\int \psi^+_{A-1}(p_2,\ldots,p'_i,p'_j,\ldots,p_A)\frac{f^{NN}(p'_j-p_j)}{\Delta_j-(p'_{jz}-p_{jz})+i\epsilon} \times \frac{f^{NN}(p'_i-p_i)}{p_z^m+\Delta-p_{1z}+i\epsilon}j^\mu(p_1,q)\psi_A(p_1,\ldots,p_i,p_j,\ldots,p_A) \times \frac{d^3p_1}{(2\pi)^3}\frac{d^3p_j}{(2\pi)^3}\frac{d^3p'_j}{(2\pi)^3}, d^3p_2,\ldots'' \ldots, d^3p_A\,, \tag{69}$$

where "$''$" in the integration means that it does not contain $d^3p_i d^3p_j$.

9.4. *Relation to the Glauber theory*

It is interesting to see how the second order rescattering amplitude derived within the GEA is related to the conventional Glauber theory. For this, it is convenient to consider the double rescattering amplitude in coordinate space. Similar to the case of single rescattering, we use coordinate space representation of nucleon propagators (as in Eq. (45)) as well as the wave function of ground and final states. Separating the c.m. and relative coordinates of the recoiled two nucleon system (see for details Ref. 62) for Eq. (68) one obtains

$$\hat{A}_2^\mu = \int d^3x_1 d^3x_2 d^3x_3 \phi_A(x_1,x_2,x_3)F_1^{\rm em}(Q^2)\mathcal{O}^{(2)}(z_1,z_2,z_3,\Delta_0,\Delta_2,\Delta_3) \times \Gamma^{NN}(x_2-x_1,\Delta_0)\Gamma^{NN}(x_3-x_1,\Delta_0)e^{-i\frac{3}{2}\mathbf{x}_1\cdot\mathbf{p}_m}\phi^\dagger(x_2-x_3)\,, \tag{70}$$

where the profile functions Γ_{NN} are defined as in Eq. (47) and we introduce the $\mathcal{O}$ function which accounts for the geometry of two sequential rescatterings as

$$\mathcal{O}^{(2)}(z_1,z_2,z_3,\Delta_0,\Delta_2,\Delta_3) = \Theta(z_2-z_1)\Theta(z_3-z_2)e^{-i\Delta_3(z_2-z_1)}e^{i(\Delta_3-\Delta_0)(z_3-z_1)} + \Theta(z_3-z_1)\Theta(z_2-z_3)e^{-i\Delta_2(z_3-z_1)}e^{i(\Delta_2-\Delta_0)(z_2-z_1)}\,. \tag{71}$$

In the conventional Glauber theory, $\mathcal{O}$ corresponds to $\Theta(z_2 - z_1)\Theta(z_3 - z_1)$ which has a simple geometrical interpretation of sequential rescattering of the knock-out nucleon on the two spectator nucleons in the target. It ensures that the rescattering cannot happen with the nucleons which are located before the knocked-out nucleon. However, the account for the finite momenta of target nucleons complicates the simple picture in the Glauber theory and the result is Eq. (71). It is important to note that in the limit of the small Fermi momenta:

$$\mathcal{O}|_{\Delta,\Delta_2,\Delta_3\to 0} \to \Theta(z_2 - z_1)\Theta(z_3 - z_1)\,. \tag{72}$$

To summarize the result of the calculation of double rescattering amplitude, we would like to point out that generalization of the Glauber theory corresponds to the modification of profile functions according to Eq. (47) as well as generalization of the product of Θ functions to the $\mathcal{O}$ function of Eq. (71).

9.5. *The case of $A > 3$ nuclei*

Generalization of the scattering amplitude for the case of multiple rescatterings is straightforward[62]:

$$\hat{T}^{(n)}_{\rm FSI} = \sum_{i,j,\ldots,n=2;i\neq j\neq\cdots n}^{A} \mathcal{O}^{(n)}(z_1, z_i, z_j, \ldots, z_n, \Delta_0, \Delta_i, \Delta_j, \ldots, \Delta_n) \times \Gamma^{NN}(x_i - x_1, \Delta_0)\Gamma^{NN}(x_j - x_1, \Delta_0)\cdots\Gamma^{NN}(x_n - x_1, \Delta_0)\,, \tag{73}$$

where

$$\mathcal{O}^{(n)}(z_1, z_i, z_j, \ldots, z_n\Delta_0, \Delta_i, \Delta_j, \ldots, \Delta_n) = \sum_{\rm perm} \Theta(z_i - z_1)\Theta(z_j - z_i)\cdots\Theta(z_n - z_{n-1}) e^{i(\Delta_0 - \Delta_j - \cdots\Delta_n)(z_i - z_1)} \times e^{i\Delta_j(z_j - z_1)}\cdots e^{i\Delta_n(z_n - z_1)} e^{-i\Delta_0(z_i + z_j + \cdots z_n - n\times z_1)}\,. \tag{74}$$

The sum in Eq. (74) goes over all permutations between $i, j, \ldots, n$. We would like to draw attention to the fact that the contribution of diagrams where the ejected nucleon interacts with, say, nucleon "2" then with nucleon "3" and then again with nucleon "2" is exactly zero. In a coordinate representation this follows from the structure of the product of Θ-functions. In the momentum representation this follows from the possibility of closing the contour of integration in the complex plane without encountering nucleon poles (see e.g. the discussion in Sec. II.C of Ref. 88 and the proof of the reduction theorem in Sec. VI.2).

It is easy to check that in the case of small excitation energies, i.e. (Δ_0, Δ_i, $\Delta_j, \ldots, \Delta_n \to 0$):

$$\mathcal{O}^{(n)}(z_1, z_i, z_j, \ldots, z_n, \Delta_0, \Delta_i, \Delta_j, \ldots, \Delta_n)|_{\Delta_0,\Delta_{i,k,n}\to 0} \Rightarrow \Theta(z_i - z_1)\Theta(z_j - z_1)\cdots\Theta(z_n - z_1)\,, \tag{75}$$

and Eq. (73) is reduced to the conventional form of the Glauber approximation, with a simple product of the Θ-functions. Within this particular approximation the sum over all n-fold rescattering amplitudes can be represented in the form of an optical potential.

However, in many cases in high-energy $(e, e'N)$ reactions the excitation energies are not too small. The use of the $\mathcal{O}^{(n)}(z_1, z_i, z_j, \ldots, z_n, \Delta_0, \Delta_i, \Delta_j, \ldots, \Delta_n)$, defined within the GEA according to Eq. (74) instead of a simple product of Θ functions is the generalization of the nonrelativistic Glauber approximation to the processes where comparatively large excitation energies are important.

The practical consequence of the difference between $\mathcal{O}^{(n)}$ and the usual Θ functions is that for sufficiently large excitation energies the sum of n-fold rescatterings differs substantially from the simple optical model limit. To illustrate the deviations from the conventional Glauber approximation (which is expressed using a simple product of the Θ functions) in Fig. 21 we compare $\mathcal{O}^{(2)}(z_1, z_2, z_3, \Delta_0, \Delta_1, \Delta_2)$ with $\Theta(z_2 - z_1)\Theta(z_3 - z_1)$ for $(e, e'p)$ scattering off a ^{3}He target. We use the kinematics for three body breakup in the final state. Figure 21 demonstrates a considerable deviation between $\mathcal{O}^{(2)}$ and the product of Θ-functions, already at comparatively low excitation energies.

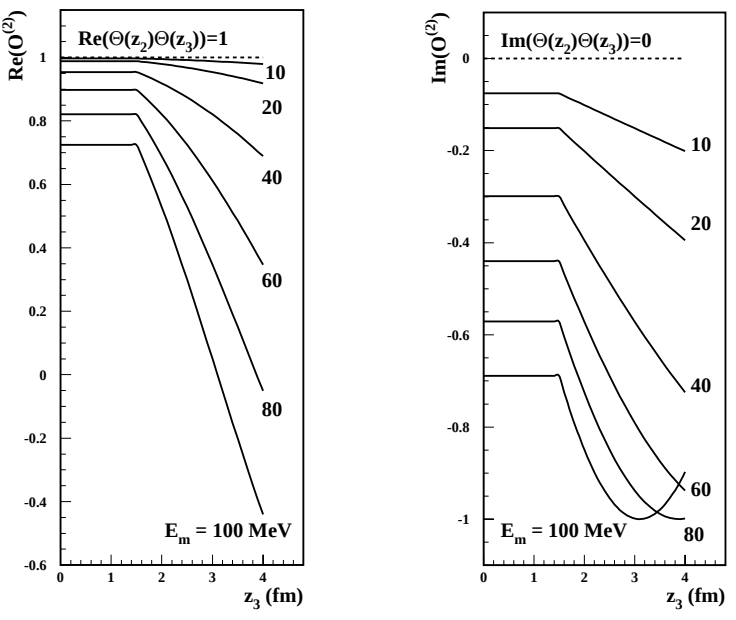

(a) (b)

Fig. 21. Dependence of $\mathcal{O}^{(2)}(z_1, z_2, z_3, \Delta_0, \Delta_1, \Delta_2)$ and $\Theta(z_2 - z_1)\Theta(z_3 - z_1)$ on z_3 for different values of missing energy E_m for $z_1 = 0$, $z_2 = 1.5$ Fm and $\Delta_1 = \Delta_2 = 0$. (a) Comparison of Re $\mathcal{O}^{(2)}(\cdots)$ (solid line) with Re $\Theta(z_2 - z_1)\Theta(z_3 - z_1) = 1$ (dashed line) and (b) comparison of Im $\mathcal{O}^{(2)}(\cdots)$ (solid line) with Im $\Theta(z_2 - z_1)\Theta(z_3 - z_1) = 0$ (dashed line).

For example, the real parts differ by more than 20% already for $\sim$ 60 MeV, leading to a comparable difference of the double rescattering amplitude calculated including effects of longitudinal momentum transfer. The detailed numerical studies of these effects for $A = 3$ nuclei are in progress.

The comparisons in Fig. 21 shows also that for light nuclei the conventional Glauber approximation, which neglects nuclear Fermi motion, is applicable only in the case of small values of excitation energies of the residual nuclei.

10. FSI and the Study of Short-Range Nucleon Correlations in Nuclei

In this section we discuss how the GEA allows us to gain an additional insight into the problem of the studies of short range correlations (SRC) in nuclei.

It is generally believed that the experimental condition $|\mathbf{p}_m| = |\mathbf{p}_f - \mathbf{q}| > k_{\rm F}$, (where $k_{\rm F} \sim 250$ MeV/c is the momentum of the Fermi surface for a given nucleus) will enhance the contribution to the cross-section from the short-range nucleon correlations in the nuclear wave function. However, the simple impulse approximation relation (Eq. (58)) is, in general, distorted by the FSI, which, in average, is sensitive to the long range distances in nuclei. Let us denote the internal momentum of the knock-out nucleons prior to the collision as $\mathbf{p}_1(p_{1z}, p_{1t})$. It follows from Eqs. (59) and (69) that

$$\mathbf{p}_{1t} = \mathbf{p}_{mt} - \mathbf{k}_t \,, \tag{76}$$

where $\mathbf{p}_{mt}$ is the transverse component of the measured missing momentum, and k_t is the momentum transferred in rescattering. The average $\langle \mathbf{k}_t^2 \rangle \sim 0.25$ GeV^2 in the integral over k_t; it is determined by the slope of the NN amplitude. The longitudinal component of the nucleon momentum in the initial state can be evaluated through its value at the pole of the rescattered nucleon propagator (see e.g. Eqs. (41), (59) and (69)):

$$p_{1z} = p_m^z + \Delta_0 \,, \tag{77}$$

where p_m^z is the longitudinal component of the measured missing momentum and Δ_0 is proportional to the excitation energy of the residual nuclear system (see Eqs. (42), (60) and (61)) and is always positive. Thus, if the measured $p_{zm} > k_{\rm F}$ then, p_{1z} is even larger, i.e. $(p_{z1} > p_{zm})$ and therefore the FSI amplitude is as sensitive to the short range correlations as the IA amplitude. In particular, within the approximation, where the high-momentum component of the nuclear spectral function is due to two-nucleon short-range correlations (see e.g. Refs. 47 and 89), the condition $p_{zm} > k_{\rm F}$ corresponds to projectile electron scattering off the forward moving nucleon of the two-nucleon correlation accompanied by the emission of the backward nucleon.

The situation is the opposite if the measured momentum $p_{zm} < -k_{\rm F}$. It follows from Eq. (77), that in this case the momenta in the wave function contributing to the rescattering amplitude are smaller than those for IA: $|p_1^z| = |p_m^z| - \Delta_0 < |p_m^z|$.

Experimentally, this situation corresponds to the forward nucleon electroproduction at $Q^2/2mq_0 \equiv x > 1$. An important new feature in this case is that in exclusive electro-production the value of Δ_0 is measured experimentally and can be easily chosen so that momenta entering in the ground state wave function would be larger than $k_{\rm F}$. Therefore to investigate the short-range correlations in the $(e, e'p)$ reactions for $x > 1$, we have to impose an additional condition:

$$p_m^z - \Delta_0 > k_{\rm F} \tag{78}$$

to suppress the contribution from large inter-nucleon distances. The appearance of this constraint is the result of the GEA and cannot be deduced within the conventional Glauber approximation.

There are several experimental projects which will be able to check the prediction on the possibility of suppression of FSI at $x > 1$ kinematics.[66–69,90–94] The most basic experiments are the electro-disintegration of the deuteron[66–69] which will allow the measurement of the angular dependence of the transparency, T as it was defined in Eq. (52) and check on the features discussed in the Sec. 8.4, Figs. 14 and 15. These experiments will also allow the verification of the expectation that with increasing energies the qualitative changes discussed in Secs. 3–6 occur.

The experiments on high momentum transfer electro-disintegration of $A = 3$ nuclei[90,91] with large values of missing momenta and energy are important to verify the applicability of the GEA for higher order of rescatterings. These measurements, which are currently in the stage of data analyses, will allow one to identify the regions where FSI is suppressed thereby allowing one to gain rather direct information about the short range structure of few-body nuclear systems.

The possibility of suppression of FSI in the $x < 1$ and $x > 1$ regions will be explored in the experiments of Refs. 92 and 93, in which the attempt to extract the direct information about short-range, few-nucleon correlations in semi-exclusive $A(e, e'NN)X$ reactions will be made.

Another interesting possibility is the study of the structure of FSI in high-energy two-body break-up processes in $^4{\rm He}(e, e'p)^3{\rm H}$ reactions. The momentum distribution for these reactions calculated within PWIA exhibits a minimum (node) at $p_m \approx 420$ MeV/c.

It is because the selection rules on angular momentum and parity requires only the S-wave to contribute in the two-body break-up amplitude of $^4{\rm He}(e, e'p)^3{\rm H}$ reactions. The minimum in the S-wave exists only if the NN correlation is included in considerations. The lack of the minimum in the experimental distribution measured in Ref. 95 at initial electron energies 0.525 GeV is correctly attributed to FSI, MEC and IC contributions (see Fig. 22). If the minimum is indeed there then one expects that with an increase in energy these reactions, measured in parallel and perpendicular kinematics, can be an important tool for studying the structure of FSI. The naive estimation[94] of the effects of FSI within the GEA for $^4{\rm He}(e, e'p)^3{\rm H}$ reactions at $Q^2 = 1$ GeV^2 shows that one may expect qualitative differences between momentum distribution in parallel, antiparallel and perpendicular kinematics (Fig. 23).

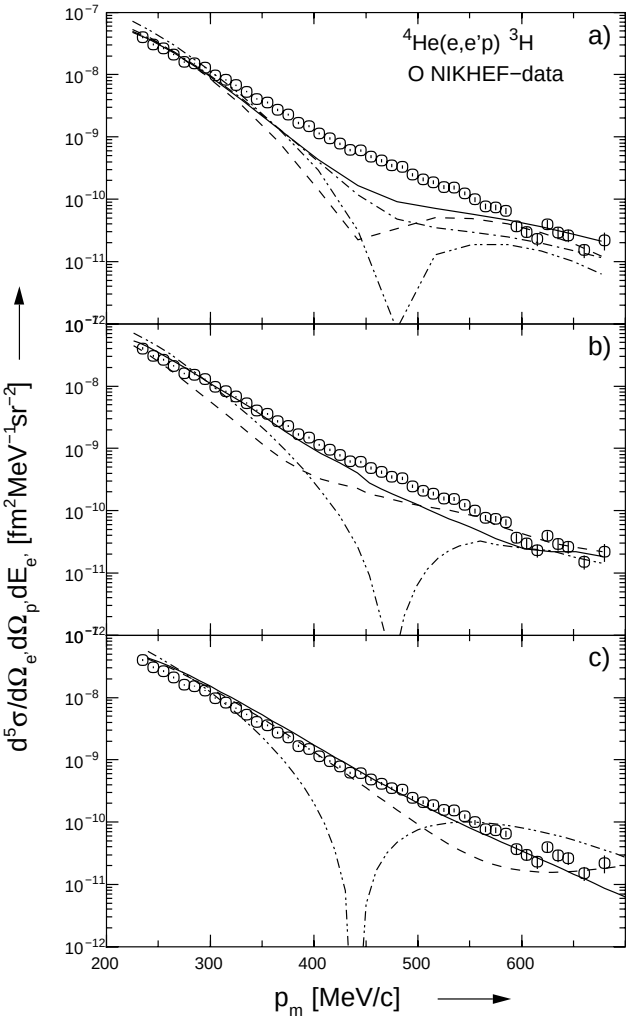

Fig. 22. Differential ^{4}He$(e, e'p)^3$H cross-section as a function of the missing momentum p_m. The calculations, in (a) according to Ref. 96 (dotted: PWIA, dashed: +FSI, dot-dashed: +two-body MEC, solid: + three-body MEC), in (b) according to Ref. 97 (dotted: PWIA, dashed: +FSI, solid: + two-body currents), and in (c) according to Ref. 98 (dotted: PWIA, dashed: tree-type diagrams, solid: + one-loop diagrams). The figure is from Ref. 95.

Note that the calculations of Fig. 23 are by no means to be considered complete since the GEA is implemented using simple harmonic oscillator wave functions for the rescattering amplitudes. Also, only the imaginary part of the NN scattering amplitudes is taken into account. The realistic wave function in these calculations is used only for the PWIA contribution.

Recent calculations of ^{4}He$(e, e'p)^3$H reactions using realistic wave functions in all rescattering amplitudes[99,100] within the conventional Glauber approximation

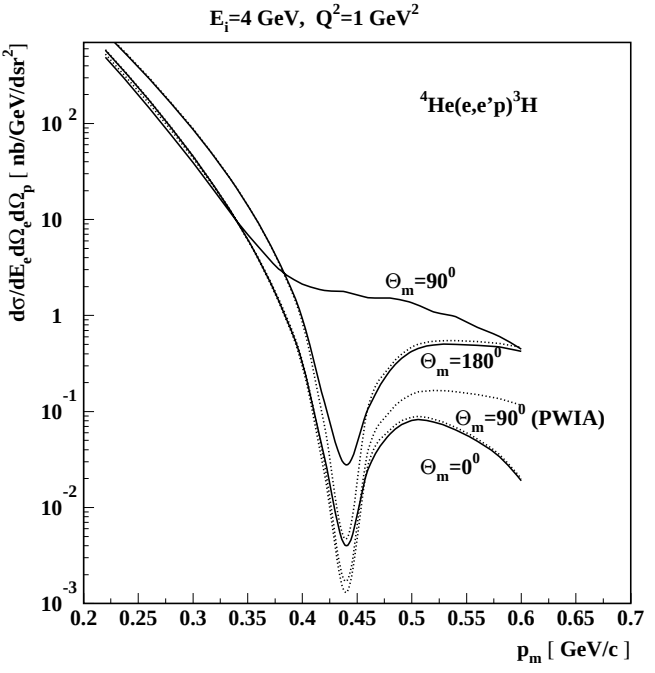

Fig. 23. Differential ^{4}He$(e,e'p)^3$H cross-section as a function of the missing momentum p_m at different values of missing momentum angles with respect to $\mathbf{q}$. (Dotted: PWIA prediction, solid: PWIA+FSI.) Note that the nonzero values of minima in PWIA curves are the result of the finite resolution of p_m implemented in calculation.

also demonstrated the large differences between the momentum dependence of the cross-section at different angles. However, Ref. 99 predicts that some signature of the minimum should still be visible after taking into account for FSI while Ref. 100 predicts a complete disappearance of the minimum both for parallel and antiparallel kinematics. Thus, the experimental data being analyzed in Ref. 94 will be of utmost importance.

11. Emergence of Light-Cone Dynamics

The obtained results within the GEA have a simple explanation in terms of the light-cone dynamics of high-energy scattering processes. Indeed, according to Eqs. (42), (60) and (61) Δ_0 does not disappear with an increase in energy. Hence, the non-conservation of the longitudinal momentum of nucleons given by Eq. (77): $p_{1z} - p_m^z = \Delta_0$ remains finite in the high-energy limit. However, the rescattering of an energetic knock-out nucleon practically does not change the "$-$" component of its four-momentum $p_- \equiv E - p_z$, (recall that p_- is the longitudinal momentum as defined in light-cone variables, where $p^\mu \equiv (p_+, p_-, p_t)$ with $p_\pm = E \pm p_z$). Really, if we define $p_{1-} = m - p_{1z}$ and $p_{m-} = p_{f-} - q_- = m - E_m - p_{mz}$, where $E_m = m + E_{A-1} - M_A$ is the missing energy, then according to Eq. (77) the

non-conservation of the "−" component is

$$p_{1-} - p_{m-} \approx \frac{Q^2}{2q^2} E_m = \frac{E_m}{2\left(1+\frac{q_0}{2mx}\right)}\,. \tag{79}$$

It vanishes with increasing virtual photon energy q_0. Hence, the physical interpretation of Eq. (77) is that, at high energies, elastic FSI does not noticeably change the light-cone "−" component of the struck nucleon momentum. This result is in agreement with our observation in Sec. 6.1. This reasoning indicates that the description of FSI in high-energy processes should be simplified when treated within the framework of the light-cone dynamics. Our previous analysis of $x > 1$, large Q^2 data on inclusive (e, e') processes is consistent with this idea.[101]

The above observation helps to rewrite the deduced formulae in a form accounting, in a straightforward way, for the fact that high-energy processes develop along the light-cone. One uses the previously introduced light-cone momenta $\alpha_i \equiv A\frac{p_{i-}}{P_{A-}}$. Here α_i/A is a momentum fraction of the target nucleus carried by the nucleon-i. Using the expressions discussed above for p_{m-} and p_{1-} and Eqs. (59), (60) and (61) for the propagator of a fast nucleon we obtain

$$\frac{1}{[p_z^m + \Delta_0 - p_{1z} + i\epsilon]} = \frac{1}{m[\alpha_1 - \alpha_m + \frac{q_0-q}{qm}E_m + i\epsilon]} \approx \frac{1}{m[\alpha_1 - \alpha_m - \frac{Q^2}{2q^2}\frac{E_m}{m} + i\epsilon]}\,. \tag{80}$$

In the kinematics where relativistic effects in the wave function of the target and residual nucleus are small and $\alpha_j \approx 1 - \frac{p_{jz}}{m}$, there is a smooth correspondence between nonrelativistic and light-cone wave functions of the nucleus,[47] i.e. $\phi_A(p_1, \ldots, p_j, \ldots, p_A) \approx \phi_A(\alpha_1, p_{1t}, \ldots, \alpha_j, p_{jt}, \ldots, \alpha_A, p_A)/m^{\frac{A}{2}}$. Therefore the amplitude of single rescattering, Eq. (47) can be rewritten as

$$T^{(b)} = -\frac{\sqrt{(2\pi)^3}(2\pi)^3}{2m}\int \psi_A(\alpha_1, p_{1t}, \alpha_2, p_{2t}, \alpha_3, p_{3t}) F_1^{\rm em}(Q^2)$$
$$\times \frac{f^{NN}}{[\alpha_1 - \alpha_m - \frac{Q^2}{2q^2}\frac{E_m}{m} + i\epsilon]} \psi_{A-1}(\alpha_2', p_{2t}', \alpha_3, p_{3t}) \frac{d\alpha_1 d^2p_{1t}}{(2\pi)^3}\frac{d\alpha_3 d^2p_{3t}}{(2\pi)^3}\,, \tag{81}$$

where, according to Eq. (63), $\alpha_2 = \alpha_2' = 3 - \alpha_1 - \alpha_3$. Equation (81) shows that in the limit when $\frac{Q^2}{2q^2}\frac{E_m}{m} \to 0$, the amplitude $T^{(b)}$ is expressed through the light-cone variables and the light-cone wave functions of the nucleus. Note that the eikonal scattering corresponds to the linear (in α_1) propagator of the fast nucleon. It is instructive that the regime of the light-cone dynamics is reached in Eq. (81) at relatively moderate energies. Indeed, let us consider kinematics when α_1 is close to unity, (which is the case in our analysis). At $q_0 \sim 2$ GeV, $\frac{Q^2}{2q^2}\frac{E_m}{m} = \frac{1}{2(1+\frac{q_0}{2mx})}\frac{E_m}{m} \sim (0.05 - 0.07) \ll 1$. As an estimate, we take $x = 1$ and for missing energy $E_m \sim 0.2 - 0.3$ GeV, which is close to the limit of applicability of the description of nuclei as a many-nucleon system (see e.g. Ref. 56). Similar reasoning is applicable for the double rescattering amplitude in Eq. (67). Here, we obtain

$$T^{(d)} = \frac{\sqrt{(2\pi)^3}(2\pi)^3}{4m^2}\int \psi_A(\alpha_1, p_{1t}, \alpha_2, p_{2t}, \alpha_3, p_{3t}) F_1^{\rm em}(Q^2)$$
$$\times \frac{f^{NN}(p_{1t} - p_{mt} - (p'_{3t} - p_{3t}))}{[\alpha_1 - \alpha_m - \frac{Q^2}{2q^2}\frac{E_m}{m} + i\epsilon]} \frac{f^{NN}(p'_{3t} - p_{3t})}{[\alpha_3 - \alpha'_3 - \frac{Q^2}{2q^2}\frac{k^2_{3t}}{2m^2} + i\epsilon]}$$
$$\times \psi_{A-1}(\alpha_2, p'_{2t}, \alpha_3, p'_{3t}) \frac{d\alpha d^2p_{1t}}{(2\pi)^3}\frac{d\alpha_3 d^2p_{3t}}{(2\pi)^3}\frac{d\alpha'_3 d^2p'_{3t}}{(2\pi)^3}\,. \qquad (82)$$

Another interesting consequence of the representation of the scattering amplitude through the light-cone variables, is the simple form of the closure approximation for the sum over the residual $(A-1)$ nuclear states in the $A(e,e'N)(A-1)$ reaction. When summing over E_m at fixed p_m the rescattering amplitudes (e.g. Eq. (47)) could not be factored out from the sum because they depend on E_m through the Δ factors (Eqs. (42), (60) and (61)). In the case of the light-cone representation (e.g. Eq. (81)) the analogous procedure[56] is to sum over $p_+ \approx m + E_m + p_{mz}$ at fixed α_m. It follows from Eq. (81) that in such a sum the scattering amplitude is independent of p_+ and therefore the application of closure has a simple form.

Note that the present discussion of the light-cone dynamics is by no means complete, since we do not consider the relativistic effects in the description of the nuclear wave functions. The extension of the current analysis to the light-cone formalism will be presented elsewhere.

12. Conclusions

The increase in transferred energies provides a qualitative new regime in electro-nuclear reactions. The possibility of suppressing the long-range phenomena in these reactions opens a completely new window in the study of microscopic properties of nuclear matter at small distances.

We give arguments why, with the increase in transferred energies, the description of semi-exclusive electro-nuclear reactions should simplify. However, in this regime the theoretical methods of low/intermediate energy electro-nuclear reactions become inapplicable. The theoretical approach which allows us to do consistent calculation is based on the fact that in the high energy regime new small parameters (such as $\frac{q_-}{q_+}$) emerge (Sec. 2). We demonstrate how the existence of these parameters reveals several new features in electro-nuclear reactions such as: the on-shellness of the "good" component of the electromagnetic current of the bound nucleon, the onset of a new approximate conservation law for high-energy small angle rescatterings, and the existence of a reduction theorem which allows one to group a potentially infinite number of rescattering amplitudes into a finite number of covariant amplitudes.

Furthermore, we identify the set of effective Feynman diagram rules which allow one to calculate these covariant amplitudes. We call this framework the generalized eikonal approximation (GEA).

The GEA provides a natural framework for generalization of the conventional Glauber approximation to high-energy processes with large values of missing momenta and energy in the reaction. This approach adequately describes the relativistic dynamics characteristic to high-energy reactions.

To demonstrate the application of the GEA, we first calculate the high energy electro-disintegration of the deuteron. Furthermore, we discuss the electro-disintegration of $A = 3$ targets and generalize the obtained formulae for the case of large A nuclei. It follows from these considerations that the formulae of the conventional Glauber approximation are a limiting case of the GEA at small values of missing momenta and energy.

Analyzing the obtained formulae for final state reinteractions, we identify the kinematic domains preferable for investigation of short-range nucleon correlations in nuclei. We find a new kinematic condition: $p_m^z - \Delta_0 > k_{\rm F}$, for semi-exclusive reactions to enhance the contribution of short-range nucleon correlations at $x > 1$ and reduce the FSI.

We also observe that the dominance of light-cone dynamics follows directly from the analysis of the Feynman diagrams, and that the "$-$" component of the target nucleon momentum is almost conserved in FSI. Therefore, by measuring the "$-$" component of missing momenta, we directly tag the pre-existing momenta in the light-cone nuclear wave function. In the end we demonstrate how simple the rescattering amplitudes are expressed through the light-cone momenta, and most importantly, the missing energy (defined in the light-cone) dependence is factorized from the rescattering amplitudes. This observation has a significant consequence for the application of the closure approximation in the discussion of FSI in high energy inclusive (e, e') reactions.

Finally, we briefly reviewed the ongoing and planned experiments on high-energy semi-exclusive reactions. Emerging experimental data on these reactions within the next several years will significantly contribute to the understanding of the dynamics of high-energy electro-nuclear reactions as well as provide an unprecedented quality of data for the investigation of nuclear structure at small internucleon distances.

13. Acknowledgments

I would like to thank L. L. Frankfurt, G. A. Miller and M. I. Strikman for fruitful collaboration and for useful discussions and suggestions during the period of writing this review. Special thanks to E. Henley for the suggestion to write this review and for very valuable comments on the text. This work is supported by a DOE grant under contract DE-FG02-01ER-41172.

I also gratefully acknowledge a contract from Jefferson Lab under which this work was done. The Thomas Jefferson National Accelerator Facility (Jefferson Lab) is operated by the Southeastern Universities Research Association (SURA) under DOE contract DE-AC05-84ER40150.

Appendix A: Why Closure Approximation has Wider Region of Applicability in the Light-Cone Compared to the Nucleus Rest Frame

In the calculation of the n-fold rescattering amplitude of Fig. 12 we assumed the decoupling (from the excitation energies of intermediate states) of the propagator of the high-energy knocked-out nucleon: $D(p_1+q)^{-1}$. Such a decoupling allows us to use the closure over the sum over the excitations of intermediate nuclear states. As a result the scattering amplitude in Eq. (28) is calculated in terms of the propagators of free spectator nucleons in the intermediate states.

To visualize the conditions when the decoupling of the high-energy part of the diagram of Fig. 12 from the low-energy part would be valid, we consider two reference frame descriptions: Nucleus rest frame (Lab frame) and Light-Cone.

In the Lab frame the inverse propagator of energetic knocked-out nucleon: $-D(p_1+q) = (p_1+q)^2 - m^2 + i\epsilon$ can be written as

$$\begin{aligned}(p_1+q)^2 - m^2 &= p_1^2 + 2E_1 q_0 - 2\mathbf{p}_1\cdot\mathbf{q} + q^2 - m^2 \\ &= 2|\mathbf{q}|\left[\frac{p_1^2-m^2}{2|\mathbf{q}|} + E_1\frac{q_0}{|\mathbf{q}|} - p_{1z} - \frac{Q^2}{|2\mathbf{q}|}\right]. \qquad \text{(A1)}\end{aligned}$$

It follows from the right-hand side of Eq. (A1) that only the term $E_1\frac{q_0}{|\mathbf{q}|} - p_{1z}$ survives in the limit of large momentum transfer ($\mathbf{q}$) and fixed x_{Bj}. Thus, in the high-energy limit within the Lab frame description one should retain the dependence of the propagator on the excitation energy of the intermediate state (via E_1). Therefore, unless the E_1 dependence of the propagator of the knocked-out nucleon can be neglected, the use of closure over the intermediate nuclear states cannot be justified. In the Lab frame description such a neglection is legitimate in the nonrelativistic limit only where the term $\frac{p_1^2}{2m^2} \ll 1$ is neglected everywhere in the expression for the scattering amplitude. Such a restriction on the applicability of the closure for the sum over the intermediate states is of crucial importance for the models where relativistic effects are treated on the basis of the Lab frame description.

The above calculation does not take into account additional approximate conservation law characteristics for light-cone dynamics. Let us introduce light-cone momenta for four-vectors as: $p^\mu(p_+, p_-, p_t)$, where $p_\pm = E \pm p_z$. Using these definitions, for the inverse propagator of the knocked-out nucleon one obtains

$$\begin{aligned}(p_1+q)^2 - m^2 &= p_1^2 + p_{1+}q_- + p_{1-}q_+ + q^2 - m^2 \\ &= q_+\left[\frac{p_1^2-m^2}{q_+} + p_{1+}\frac{q_-}{q_+} + p_{1-} - \frac{Q^2}{q_+}\right]. \qquad \text{(A2)}\end{aligned}$$

As follows from the above equation the only term that survives at fixed x_{Bj} and high-energy transfer limit, is p_{1-}. Therefore at fixed p_- we found effective factorization of the high-energy propagator from the low-energy intermediate nuclear part whose excitation energy on the light-cone is defined by p_{1+}.[47,56] Such a decoupling applies for any values of Fermi momenta of the target nucleon (no restriction like

$\frac{p_1^2}{2m^2} \ll 1$ is formally needed). Therefore, it is possible to extend the application of the closure over intermediate states of the residual nucleus to the domain of relativistic momenta of the target nucleons. The price is to introduce the light-cone wave functions of the target (similar to the case of pQCD).

Note that the considerations in the present work are restricted by relatively small Fermi momenta (e.g. Eq. (30)) since we use $\frac{p_1^2}{2m^2} \ll 1$ in the scattering amplitude. For larger Fermi momenta a way to generalize the obtained results is to use the light-cone description, which is beyond the scope of the present paper. Note that the light-cone mechanics of nuclei is rather similar to the nonrelativistic ones.[47,102]

Appendix B: Analytic Calculation of Rescattering Amplitude

We calculate the rescattering amplitude in Eq. (41) by the method described in Ref. 61 using the deuteron wave function in momentum space, defined as[103]

$$\psi_D^\mu(p) = \frac{1}{\sqrt{4\pi}} \left(u(p) + w(p) \sqrt{\frac{1}{8}} S(p_z, p_t) \right) \chi^\mu \,, \tag{B1}$$

where χ^μ is the deuteron spin function and

$$S(p_z, p_t) = \frac{3(\boldsymbol{\sigma}_p \cdot \mathbf{p})(\boldsymbol{\sigma}_n \cdot \mathbf{p})}{p^2} - \boldsymbol{\sigma}_p \cdot \boldsymbol{\sigma}_n \,, \tag{B2}$$

where σ_p, σ_p are Pauli matrices. The functions $u(p)$ and $w(p)$ are the radial wave functions of S- and D-states, respectively, and they can be written as[104,105]:

$$u(p) = \sum_j \frac{c_j}{p^2 + m_j^2} \,; \qquad w(p) = \sum_j \frac{d_j}{p^2 + m_j^2} \,, \tag{B3}$$

where $\sum_j c_j = \sum_j d_j = 0$, which guarantees that $u(p)$, $w(p) \sim \frac{1}{p^4}$ at large p and $\sum_j \frac{d_j}{m_j^2} = 0$ to provide $w(p=0) = 0$. The insertion of Eq. (B3) into Eq. (41) gives

$$A_1^\mu = -\frac{(2\pi)^{\frac{3}{2}} \sqrt{2E_s}}{2} \int \frac{d^2 p'_{st}}{(2\pi)^2} f^{pn}(k_t) \cdot j^\mu_{\gamma^* N} \times \int \frac{dp'_{sz}}{(2\pi)} \left(\frac{c_j}{p_s'^2 + m_j^2} + \frac{d_j}{p_s'^2 + m_j^2} \sqrt{\frac{1}{8}} S(p'_{sz}, p'_{st}) \right) \frac{\chi^\mu}{p'_{sz} - p_{sz} + \Delta + i\epsilon} \,. \tag{B4}$$

Substituting $p_s'^2 + m_j^2 = (p'_{sz} + i\sqrt{m_j^2 + p_{st}'^2})(p'_{sz} - i\sqrt{m_j^2 + p_{st}'^2})$ one can perform the integration over p'_{sz} by closing the contour in the upper p'_{sz} complex semi-plane. Note that the p^{-2} dependence of the tensor function $S(p)$ will not introduce a new singularity, since $w(p=0) = 0$. Setting the residue at the point $p'_{sz} = i\sqrt{m_j^2 + p_{st}'^2}$,

we obtain:

$$A_1^\mu = -\frac{i(2\pi)^{\frac{3}{2}}\sqrt{2E_s}}{2}\int \frac{d^2p'_{st}}{(2\pi)^2} f^{pn}(k_t)\cdot j^\mu_{\gamma^* N}\left[\frac{c_j}{2i\sqrt{p'^2_{st}+m_j^2}}\right.$$

$$\left. + \frac{d_j}{2i\sqrt{p'^2_{st}+m_j^2}}\sqrt{\frac{1}{8}}S(i\sqrt{p'^2_{st}+m_j^2}, p'_{st})\right]\frac{\chi^\mu}{i\sqrt{p'^2_{st}+m_j^2}-p_{sz}+\Delta}\,. \quad \text{(B5)}$$

After regrouping of the real and imaginary parts, the above equation can be rewritten as

$$A_1^\mu = -\frac{(2\pi)^{\frac{3}{2}}\sqrt{2E_s}}{4i}\int \frac{d^2k_t}{(2\pi)^2} f^{pn}(k_t)\cdot j^\mu_{\gamma^* N}(\psi^\mu(\tilde{p}_s) - i\psi'^\mu(\tilde{p}_s))\,, \quad \text{(B6)}$$

where $\tilde{p}_s(\tilde{p}_{sz}, \tilde{p}_{s\perp}) \equiv \tilde{\mathbf{p}}_s(p_{sz}-\Delta, \mathbf{p}_{st}-\mathbf{k}_t)$, ψ^μ is the wave function defined in Eq. (B1) and ψ'^μ is defined as

$$\psi'^\mu(p) = \left(u_1(p)p_z + \frac{w_1(p)p_z}{\sqrt{8}}S(p_z,p_t) + \frac{w_2(p)}{\sqrt{8}p_z}[S(p_z,p_t)-S(0,p_t)]\right)\chi^\mu\,, \quad \text{(B7)}$$

where

$$u_1(p) = \sum_j \frac{c_i}{\sqrt{p_t^2+m_j^2}(p^2+m_j^2)}\,, \quad w_1(p) = \sum_j \frac{d_i}{\sqrt{p_t^2+m_j^2}(p^2+m_j^2)}\,,$$

$$w_2(p) = \sum_j \frac{d_i}{\sqrt{p_t^2+m_j^2}m_j^2}\,. \quad \text{(B8)}$$

Note that the last term in Eq. (B7) does not have a singularity at $p_z = 0$ since $(S(p_z,p_t)-S(0,p_t)) \sim p_z$.

References

1. R. P. Feynman, *Photon Hadron Interactions* (Benjamin Inc., 1972).
2. H. Cheng and T. T. Wu, *Expanding Protons: Scattering at High-Energies* (MIT-PR Cambridge, USA, 1987).
3. "Program Advisory Committee" at Jefferson Lab, Newport News, VA http://www.jlab.org/exp_prog/PACpage/index.html.
4. C. Bochna *et al.*, [E89-012 Collaboration], *Phys. Rev. Lett.* **81**, 4576 (1998).
5. H. J. Bulten *et al.*, *Phys. Rev. Lett.* **74**, 4775 (1995).
6. N. Makins *et al.*, [NE18 collaboration], *Phys. Rev. Lett.* **72**, 1986 (1994).
7. T. G. O'Neill *et al.*, [NE18 collaboration], *Phys. Lett.* **B351**, 87 (1995).
8. D. Abbott *et al.*, *Phys. Rev. Lett.* **80**, 5072 (1998).
9. K. Garrow *et al.*, arXiv:hep-ex/0109027 (2001).
10. N. Liyanage *et al.*, [Jefferson Lab Hall A Collaboration], *Phys. Rev. Lett.* **86**, 5670 (2001).
11. A. Airapetian *et al.*, [HERMES Collaboration], *Eur. Phys. J.* **C20**, 479 (2001).
12. G. van der Steenhoven, [HERMES Collaboration], *Nucl. Phys.* **A663**, 320 (2000).
13. K. Ackerstaff *et al.*, [HERMES Collaboration], *Phys. Rev. Lett.* **82**, 3025 (1999).

14. White Paper: "The Science Driving the 12 GeV Upgrade of CEBAF," Jefferson Lab, Newport News, VA, 2000.
15. M. Duren and K. Rith, *Phys. Bl.* **56N10**, 41 (2000).
16. C. D. Epp and T. A. Griffy, *Phys. Rev.* **C1**, 1633, (1970); F. Cannata, J. P. Dedonder and F. Lenz, *Ann. Phys. (N.Y.)* **143**, 84 (1982).
17. CEBAF Conceptual design report, Southeastern Universities Research Association, Newport News, 1990.
18. Technical Report of the HERMES Experiment, DESY, 1991 (unpublished).
19. R. J. Glauber, *Phys. Rev.* **100**, 242 (1955); *Lectures in Theoretical Physics*, v.1, eds. W. Brittain and L. G. Dunham (Interscience Publ., N.Y., 1959).
20. D. R. Yennie, in *Hadronic Interactions of Electrons and Photons*, eds. J. Cummings and D. Osborn (Academic, New York, 1971), p. 321.
21. E. J. Moniz and G. D. Nixon, *Ann. Phys. (N.Y.)* **67**, 58 (1971).
22. G. D. Alkhazov, S. L. Belostotsky and A. A. Vorobev, *Phys. Rept.* **42**, 89 (1978).
23. G. R. Farrar, L. L. Frankfurt, H. Liu and M. I. Strikman, *Phys. Rev. Lett.* **61**, 686 (1988).
24. T.-S. H. Lee and G. A. Miller, *Phys. Rev.* **C45**, 1863 (1992).
25. B. K. Jennings and G. A. Miller, *Phys. Lett.* **B318**, 7 (1993).
26. A. Kohama, K. Yazaki and R. Seki, *Nucl. Phys.* **A551**, 687 (1993).
27. L. L. Frankfurt, M. I. Strikman and M. Zhalov, *Phys. Rev.* **C50**, 2189 (1994).
28. O. Benhar *et al.*, *Phys. Rev. Lett.* **69**, 881 (1992).
29. A. S. Rinat and M. F. Taragin, *Phys. Rev.* **C52**, 28 (1995).
30. N. N. Nikolaev, A. Szczurek *et al.*, *Phys. Lett.* **B317**, 287 (1993).
31. S. Frankel, W. Frati and N. R. Walet, *Nucl. Phys.* **A580**, 595 (1994).
32. A. Bianconi, S. Boffi, D. E. Kharzeev, *Phys. Lett.* **B325**, 294, (1994).
33. E. J. Moniz, Summary Talk in PANIC-XIII, Perugia, Italy, 1993.
34. C. Ciofi degli Atti, L. P. Kaptari and D. Treleani, *Phys. Rev.* **C63**, 044601 (2001).
35. H. Morita, C. Ciofi degli Atti and D. Treleani, *Phys. Rev.* **C60**, 034603 (1999).
36. S. Jeschonnek, *Phys. Rev.* **C63**, 034609 (2001).
37. L. L. Frankfurt, M. I. Strikman and M. Zhalov, *Nucl. Phys.* **A515**, 599 (1990).
38. L. L. Frankfurt, E. J. Moniz, M. M. Sargsyan and M. I. Strikman, *Phys. Rev.* **C51**, 3435 (1995).
39. L. L. Frankfurt, G. A. Miller and M. Strikman, *Ann. Rev. Nucl. Part. Sci.* **44**, 501 (1994).
40. V. N. Gribov, *JETP* **29**, 483 (1969).
41. C. Marchand *et al.*, *Phys. Rev. Lett.* **60**, 1703 (1988); A. Bussiere *et al.*, *Nucl. Phys.* **A365**, 349 (1981).
42. K. I. Blomqvist *et al.*, *Phys. Lett.* **B424**, 33 (1998).
43. D. L. Groep *et al.*, *Phys. Rev.* **C63**, 014005 (2001).
44. H. Arenhovel, W. Leidemann and E. L. Tomusiak, *Phys. Rev.* **C52**, 1232 (1995).
45. V. R. Pandharipande and S. C. Pieper, *Phys. Rev.* **C45**, 791 (1992).
46. L. Lapikas, G. van der Steenhoven, L. Frankfurt, M. Strikman and M. Zhalov, *Phys. Rev.* **C61**, 064325 (2000).
47. L. L. Frankfurt and M. I. Strikman, *Phys. Rep.* **76**, 215 (1981).
48. Y. Surya and F. Gross, *Phys. Rev.* **C53**, 2422 (1996).
49. R. Dashen and M. Gell-Mann, *Phys. Rev. Lett.* **17**, 340 (1966).
50. V. N. Gribov, *JETP* **30**, 709 (1970).
51. F. Gross, in *Modern Topics in Electron Scattering*, eds. B. Frois and I. Sick (World Scientific, 1991), p. 219.
52. H. W. Naus, S. J. Pollock, J. H. Koch and U. Oelfke, *Nucl. Phys.* **A509**, 717 (1990).

53. T. De Forest, *Nucl. Phys.* **A392**, 232 (1983).
54. J. Speth and A. W. Thomas, *Adv. Nucl. Phys.* **24**, 83 (1997).
55. M. Frodyma *et al.*, *Phys. Rev.* **C47**, 1599 (1993).
56. L. L. Frankfurt and M. I. Strikman, *Phys. Rep.* **160**, 235 (1988).
57. P. Stoler, *Phys. Rept.* **226**, 103 (1993).
58. Y. I. Azimov, *Yad. Fiz.* **11**, 206 (1970).
59. P. D. B. Collins, *An Introduction to Regge Theory and High Energy Physics* (Cambridge University Press, Cambridge, 1977).
60. D. E. Groom *et al.* [Particle Data Group Collaboration], *Eur. Phys. J.* **C15**, 1 (2000).
61. L. L. Frankfurt, W. R. Greenberg, G. A. Miller, M. M. Sargsian and M. I. Strikman, *Z. Phys.* **A352**, 97 (1995).
62. L. L. Frankfurt, M. M. Sargsian and M. I. Strikman, *Phys. Rev.* **C56**, 1124 (1997).
63. L. Bertuchi and A. Capella, *Il Nuovo Cimento* **A51**, 369 (1967).
64. L. Bertuchi, *Il Nuovo Cimento* **A11**, 45 (1972).
65. L. L. Frankfurt and M. I. Strikman, Private Communication.
66. S. E. Kuhn and K. A. Griffioen (spokespersons), *Electron Scattering from a High Momentum Nucleon in Deuterium*, Jefferson Lab Proposal E-94-102.
67. K. Sh. Egiyan, K. A. Griffioen and M. I. Strikman (spokespersons), *Measuring Nuclear Transparency in Double Rescattering Processes*, Jefferson Lab Proposal E-94-019.
68. W. Boeglin, A. Klein and E. Voutier (spokespersons), *A Study of the Dynamics of the Exclusive Electro-Disintegration of the Deuteron*, Jefferson Lab Proposal PR-01-008.
69. P. Ulmer and M. Jones, *In-Plane Separations and High Momentum Structure in* $d(e, e'p)n$, Jefferson Lab Proposal E-94-004.
70. S. J. Brodsky and G. R. Farrar, *Phys. Rev. Lett.* **31**, 1153 (1973).
71. A. H. Mueller, *Phys. Rept.* **73**, 237 (1981).
72. L. Frankfurt, G. A. Miller and M. Strikman, *Nucl. Phys.* **A555**, 752 (1993).
73. S. J. Brodsky, in *Proceedings if Thirteenth Intl. Symposium on Multiparticle Dynamics*, eds. W. Kittel, W. Metzegar and A. Stergiou (World Scientific, Singapore, 1982), p. 963.
74. A. H. Mueller, in *Proceedings if Seventeenth Rencontre de Moriond*, ed. J. Tran Thanh Van (Editions Frontieres, Gif-sur-Yvette, France, 1982), p. 13.
75. P. Jain, B. Pire and J. P. Ralston, *Phys. Rept.* **271**, 67 (1996).
76. S. J. Brodsky, L. Frankfurt, J. F. Gunion, A. H. Mueller and M. Strikman, *Phys. Rev.* **D50**, 3134 (1994).
77. L. Frankfurt, G. A. Miller and M. Strikman, *Phys. Lett.* **B304**, 1 (1993).
78. E. M. Aitala *et al.*, [E791 Collaboration], *Phys. Rev. Lett.* **86**, 4773 (2001).
79. L. L. Frankfurt, W. R. Greenberg, G. A. Miller, M. M. Sargsian and M. I. Strikman, *Phys. Lett.* **B369**, 201 (1996).
80. G. R. Farrar, H. Liu, L. L. Frankfurt and M. I. Strikman, *Phys. Rev. Lett.* **61**, 686 (1988).
81. B. K. Jennings and G. A. Miller, *Phys. Rev. Lett.* **69**, 3619 (1992).
82. L. Frankfurt, W. R. Greenberg, G. A. Miller and M. Strikman, *Phys. Rev.* **C46**, 2547 (1992).
83. N. N. Nikolaev, A. Szczurek, J. Speth, J. Wambach, B. G. Zakharov and V. R. Zoller, *Nucl. Phys.* **A567**, 781 (1994).
84. B. Z. Kopeliovich, *Sov. J. Nucl. Phys.* **55**, 752 (1992).
85. M. A. Braun, C. Ciofi degli Atti and D. Treleani, *Phys. Rev.* **C62**, 034606 (2000).
86. L. Frankfurt, G. A. Miller and M. Strikman, *Comments Nucl. Part. Phys.* **21**, 1 (1992).

87. L. Frankfurt, T. S. H. Lee, G. A. Miller and M. Strikman, *Phys. Rev.* **C55**, 909–916 (1997).
88. L. Frankfurt, E. Piasetzky, M. Sargsian and M. Strikman, *Phys. Rev.* **C56**, 2752 (1997).
89. C. Ciofi degli Atti, L. Frankfurt, S. Simula and M. Strikman, *Phys. Rev.* **C44**, 7 (1991).
90. W. Bertozzi, W. Boeglin and L. Weinstein (spokespersons), *Coincidence Reaction Studies with the LAS*, Jefferson Lab Proposal PR-89-015.
91. M. Epstein, A. Saha and E. Voutier (spokespersons), *Selected Studies of the 3He and 4He Nuclei through Electrodisintegration at High Momentum Transfer*, Jefferson Lab Proposal E-89-044.
92. E. Egiyan (spokesperson), *Study of Short-Range Properties of Nuclear Matter in Electron-Nucleus and Photon-Nucleus Interactions with Backward Particle Production using the CLAS Detector*, Jefferson Lab Proposal PR-89-036.
93. W. Bertozzi, E. Piasetzky and S. Wood (spokespersons), *Studying the Internal Small-Distance Structure of Nuclei via the Triple Coincidence* $(e, e'p + N)$ *Measurement*, Jefferson Lab Proposal E-01-015.
94. J. A. Templon and J. Mitchell (spokespersons), *Systematic Probe of Short-Range Correlations*, Jefferson Lab Proposal E-97-111.
95. J. J. van Leeuwe *et al.*, *Phys. Rev. Lett.* **80**, 2543 (1998).
96. J. M. Laget, *Nucl. Phys.* **A579**, 333 (1994).
97. R. Schiavilla, *Phys. Rev. Lett.* **65**, 835 (1990).
98. S. I. Nagorny *et al.*, *Sov. J. Nucl. Phys.* **53**, 228 (1991).
99. O. Benhar, N. N. Nikolaev, J. Speth, A. A. Usmani and B. G. Zakharov, *Nucl. Phys.* **A673**, 241 (2000).
100. M. Alvioli, M. A. Braun, C. Ciofi degli Atti, L. P. Kaptari, H. Morita and D. Treleani, nucl-th/0012019, 2000.
101. L. L. Frankfurt, M. I. Strikman, D. B. Day and M. Sargsian, *Phys. Rev.* **C48**, 2451 (1993).
102. L. L. Frankfurt, M. I. Strikman, in *Modern Topics in Electron Scattering*, eds. B. Frois and I. Sick (World Scientific, 1991).
103. G. E. Brown and A. D. Jackson, *The Nucleon-Nucleon Interactions* (North-Holland Publishing Company, 1976).
104. M. Lacombe, B. Loiseau, R. Vinh Mau, J. Cote, P. Pires and R. de Tourreil, *Phys. Lett.* **B101**, 139 (1981).
105. R. Machleidt, K. Holinde and C. Elster, *Phys. Rep.* **149**, 1 (1987).